

Cross-correlation between the curvature perturbations and magnetic fields in *pure* ultra slow roll inflation

Sagarika Tripathy,^{1,*} Debika Chowdhury,^{1,†} H. V. Ragavendra,^{2,3,4,‡} and L. Sriramkumar^{5,§}

¹*Indian Institute of Astrophysics, II Block, Koramangala, Bengaluru 560034, India*

²*Raman Research Institute, C. V. Raman Avenue, Sadashivanagar, Bengaluru 560080, India*

³*Dipartimento di Fisica e Astronomia “Galileo Galilei”,*

Università degli Studi di Padova, Via Marzolo 8, I-35131 Padova, Italy

⁴*Istituto Nazionale di Fisica Nucleare, Sezione di Padova, Via Marzolo 8, I-35131 Padova, Italy*

⁵*Centre for Strings, Gravitation and Cosmology, Department of Physics,
Indian Institute of Technology Madras, Chennai 600036, India*

Motivated by the aim of producing significant number of primordial black holes, over the past few years, there has been a considerable interest in examining models of inflation involving a single, canonical field, that permit a brief period of ultra slow roll. Earlier, we had examined inflationary magnetogenesis—achieved by breaking the conformal invariance of the electromagnetic action through a coupling to the inflaton—in situations involving departures from slow roll. We had found that a transition from slow roll to ultra slow roll inflation can lead to a strong blue tilt in the spectrum of the magnetic field over small scales and also considerably suppress its strength over large scales. In this work, we consider the scenario of *pure* ultra slow roll inflation and show that scale invariant magnetic fields can be obtained in such situations with the aid of a non-conformal coupling function that depends on the kinetic energy of the inflaton. Apart from the power spectrum, an important probe of the primordial magnetic fields are the three-point functions, specifically, the cross-correlation between the curvature perturbations and the magnetic fields. We calculate the three-point cross-correlation between the curvature perturbations and the magnetic fields in *pure* ultra slow roll inflation for the new choice of the non-conformal coupling function. In particular, we examine the validity of the consistency condition that is expected to govern the three-point function in the squeezed limit and comment on the wider implications of the results we obtain.

I. INTRODUCTION

Large-scale, coherent magnetic fields are observed in galaxies, clusters of galaxies, and even in the intergalactic medium (for reviews on magnetic fields, see Refs. [1–10]). The Fermi/LAT and HESS observations of TeV blazars suggest that the strength of the magnetic fields in the intergalactic voids is of the order of 10^{-16} G [11–17]. It may not be possible to explain the presence of magnetic fields in the intergalactic voids solely on the basis of astrophysical phenomena such as batteries (see Refs. [3, 4]; however, in this context, see Refs. [18, 19]). Hence, it seems necessary to invoke a cosmological mechanism for the primordial origin of these fields. While the Fermi/LAT and HESS observations provide a lower bound on the current strengths of the cosmological magnetic fields, the anisotropies in the cosmic microwave background (CMB) provide an upper bound. The primordial magnetic fields can induce scalar, vector, and tensor perturbations, which, in turn, can leave distinct signatures on the temperature and polarization angular power spectra of the CMB [20–26]. The CMB observations lead to an upper bound on the primordial magnetic fields to be of the order of 10^{-9} G [27–33].

As in the case of the scalar and tensor perturbations, it is natural to turn to the inflationary epoch in the early universe for the generation of magnetic fields. However, since the standard electromagnetic theory is conformally invariant, the magnetic fields generated in such a case will have a strongly blue spectrum, whose strength will be significantly suppressed during inflation. Therefore, to generate cosmological magnetic fields of observable strengths today, the conformal invariance of the electromagnetic action must be broken during inflation (see Refs. [34, 35]; for reviews in this context, see Refs. [5, 6, 8–10]). Often, this is achieved by the coupling the electromagnetic field to the inflaton, i.e. the scalar field(s) that drive inflation [36–40].

Since the detection of gravitational waves from merging binary black holes [41], there has been a tremendous interest in investigating if these black holes could have formed in the primeval universe [42–45]. If a significant number of black holes have to be produced in the early universe, then the primordial scalar power spectrum should have considerably higher power on small scales than the nearly scale invariant amplitude suggested by the anisotropies in the CMB over the large scales. In single field models of inflation involving the canonical scalar field, scalar spectra with enhanced power on small scales can be generated if the models admit a brief period of ultra slow roll during which the first slow roll parameter decreases very rapidly. While the first slow roll parameter remains small during the period of ultra slow roll, the second and higher order slow roll parameters turn large suggesting strong departures from slow roll inflation. It is known that such

* E-mail: sagarika.tripathy@iiap.res.in

† E-mail: debika.chowdhury@iiap.res.in

‡ E-mail: ragavendra.hv@pd.infn.it

§ E-mail: sriram@physics.iitm.ac.in

deviations from slow roll lead to enhanced levels of non-Gaussianities, in particular, the three-point functions (in this context, see, for example, Refs. [46–54]).

We had mentioned above that, to generate magnetic fields of observable strengths, during inflation, the conformal invariance of the electromagnetic action is usually broken by introducing a coupling to the inflaton. Recently, we had shown that, in single field models of inflation admitting a phase of ultra slow roll, there arises a challenge in generating magnetic fields of observable strengths over large scales [55, 56]. The phase of ultra slow roll is typically achieved with the help of a point of inflection in the inflationary potential. The scalar field slows down tremendously as it approaches the point of inflection, leading to the period of ultra slow roll. As a result, after the onset of ultra slow roll, the non-conformal coupling function ceases to evolve, essentially restoring the conformal invariance of the electromagnetic action. Such a behavior leads to a strongly scale dependent spectrum of the magnetic field on small scales. Also, the amplitude of the spectrum of the magnetic field is considerably suppressed over large scales.

In this work, we shall examine the effects of ultra slow roll inflation on the three-point cross-correlation between the curvature perturbations and the magnetic fields. Specifically, we shall focus on the scenario wherein ultra slow roll lasts for the *entire* duration of inflation, which we shall refer to as *pure* ultra slow roll inflation. Although such a scenario may not be considered as interesting from an observational point of view, the motivations for our investigations are twofold. Firstly, our aim will be to examine if we can construct suitable non-conformal coupling functions that can lead to a scale invariant spectrum for the magnetic field in ultra slow roll inflation. Secondly, in slow roll inflation, it is well known that there arises a consistency condition according to which the three-point functions involving the scalar and tensor perturbations can be completely expressed in terms of the two-point functions in the so-called squeezed limit wherein one of the three wave numbers is much smaller than the other two. This property can be attributed to the fact that the amplitude of the scalar and tensor perturbations freeze on super-Hubble scales. However, it is known that the strength of the curvature perturbations can grow indefinitely on super-Hubble scales when there arises an extended period of ultra slow roll. Due to the continued growth in the amplitude of the curvature perturbations, it has been shown that, in *pure* ultra slow roll inflation, the standard consistency condition governing the scalar bispectrum is violated [57–61]. Such a result raises the interesting question of whether, in similar situations, the three-point cross-correlation between the curvature perturbations and the magnetic field satisfies the expected consistency condition.

This manuscript is organized as follows. In the following section, we shall discuss the behavior of the background and the Fourier mode functions describing the curvature perturbations in specific *pure* ultra slow roll scenarios. We

shall also outline the generation of electromagnetic fields by a non-conformal coupling function that depends on the inflaton and discuss the behavior of the Fourier mode functions describing the electromagnetic vector potential. Further, we shall arrive at the power spectra of the curvature perturbations and the electromagnetic fields in these cases. In Sec. III, we shall consider a non-conformal coupling function that depends on the kinetic energy of the inflaton. We shall show that, for suitable choices of the parameters involved, such a coupling function leads to the desired scale invariant spectrum for the magnetic field in the ultra slow roll scenarios. In Sec. IV, we shall derive the third order action that describes the interaction between the curvature perturbation and the electromagnetic field for the new choice of the non-conformal coupling function. We shall also arrive at formal expressions for the contributions to the three-point cross-correlation (in Fourier space) between the curvature perturbations and the magnetic fields corresponding to the different terms in the action at the cubic order. We shall also introduce the non-Gaussianity parameter associated with the three-point cross-correlation of interest. In Sec. V, we shall calculate the three-point cross-correlation for two specific cases of pure ultra slow roll inflation and suitable values of the relevant parameters. We shall also illustrate the complete structure of the non-Gaussianity parameter and discuss the validity of the consistency condition governing the parameter in the scenarios we consider. Lastly, in Sec. VI, we shall conclude with a summary and outlook. We relegate complementary details of the computation and arguments on certain related issues to the appendices.

At this stage of our discussion, we should make a few clarifying remarks concerning the conventions and notations that we shall work with. We shall work with natural units such that $\hbar = c = 1$ and set the reduced Planck mass to be $M_{\text{Pl}} = (8\pi G)^{-1/2}$. We shall adopt the signature of the metric to be $(-, +, +, +)$. Note that Latin indices shall represent the spatial coordinates, except for k which shall be reserved for denoting the wave number. We shall assume the background to be the spatially flat Friedmann-Lemaître-Robertson-Walker (FLRW) universe described by the following line-element:

$$ds^2 = -dt^2 + a^2(t) d\mathbf{x}^2, \quad (1)$$

where t is the cosmic time and $a(t)$ denotes the scale factor. Also, an overdot and an overprime shall denote differentiation with respect to the cosmic time t and the conformal time $\eta = \int dt/a(t)$, respectively.

II. BACKGROUND, MODE FUNCTIONS AND POWER SPECTRA

In this section, we shall discuss the behavior of the background as well as the Fourier mode functions of the curvature perturbation and the electromagnetic field in ultra slow roll inflation. We shall also discuss the power spectra of the curvature perturbations and the

electromagnetic fields that arise in a couple of specific situations.

A. Evolution of the background

Recall that the equation of motion governing a homogeneous, canonical scalar field, say, ϕ , that is described by the potential $V(\phi)$ is given by

$$\ddot{\phi} + 3H\dot{\phi} + V_\phi = 0, \quad (2)$$

where $H = \dot{a}/a$ is the Hubble parameter and $V_\phi = dV/d\phi$. As we mentioned above, a brief epoch of ultra slow roll inflation is usually realized in potentials that contain a point of inflection, i.e. a point wherein the first and the second derivatives of the potential, viz. V_ϕ and $V_{\phi\phi} = d^2V/d\phi^2$, vanish (see, for instance, Refs. [50, 62, 63]). Note that, when $V_\phi = 0$, the equation of motion for the scalar field reduces to

$$\ddot{\phi} = -3H\dot{\phi}, \quad (3)$$

which can be immediately integrated to obtain that $\dot{\phi} \propto a^{-3}$. Also, the fact that $V_\phi = 0$ suggests that the Hubble parameter H is nearly a constant. In such a situation, the first slow roll parameter $\epsilon_1 = \dot{\phi}^2/(2H^2M_{\text{pl}}^2)$ behaves as

$$\epsilon_1 \propto \frac{1}{a^6}. \quad (4)$$

In this work, we shall be interested in *pure* ultra slow roll inflation, i.e. scenarios that lead to ultra slow roll for the *entire* duration of inflation. To allow for different types of evolution of the first slow parameter, we shall modify Eq. (3) and consider an equation of the form (for a detailed discussion in this regard, see Refs. [58, 64, 65])

$$\ddot{\phi} = -\frac{p}{2}H\dot{\phi}, \quad (5)$$

with $p = 6$ evidently corresponding to the original case. Clearly, this leads to $\dot{\phi} \propto a^{-p/2}$ and, for $p > 0$, the velocity as well as the acceleration of the field continue to decrease. If we assume that the initial value of the first slow roll parameter is small (say, $\epsilon_{1i} \lesssim 10^{-2}$), since it decreases rapidly thereafter, the Hubble parameter remains nearly a constant. Hence, the scale factor during ultra slow roll inflation can be expressed in the de Sitter form as $a(\eta) = -1/(H_I \eta)$, where H_I denotes the constant value of the Hubble parameter. Therefore, in such situations, we can express the first slow roll parameter as

$$\epsilon_1(\eta) = \epsilon_{1i} \left[\frac{a_i}{a(\eta)} \right]^p = \epsilon_{1i} \left(\frac{\eta}{\eta_i} \right)^p, \quad (6)$$

where ϵ_{1i} is the initial value of the first slow roll parameter when the value of the scale factor is $a_i = -1/(H_I \eta_i)$ at the conformal time η_i . In our discussion below, we shall consider two cases wherein $p = 6$ and $p = 4$. As we shall

see, the first of these leads to a scale invariant spectrum for the curvature perturbations, while the second leads to simple mode functions, which allows us to easily calculate the two and three-point functions of interest¹.

B. Mode functions describing the curvature perturbation and the scalar power spectrum

Let us now discuss the mode functions describing the curvature perturbation and the resulting scalar power spectrum in the ultra slow roll scenarios of interest. Let \mathcal{R} denote the curvature perturbation and let f_k denote the corresponding Fourier mode functions. Recall that the Fourier mode functions f_k that characterize the curvature perturbation satisfy the differential equation (see, for example, the reviews [66–75])

$$f_k'' + 2\frac{z'}{z}f_k + k^2f_k = 0, \quad (7)$$

where $z = \sqrt{2\epsilon_1}M_{\text{pl}}a$. On quantization, the curvature perturbation \mathcal{R} can be expressed in terms of the mode functions f_k as follows:

$$\begin{aligned} \hat{\mathcal{R}}(\eta, \mathbf{x}) &= \int \frac{d^3\mathbf{k}}{(2\pi)^{3/2}} \hat{\mathcal{R}}_{\mathbf{k}}(\eta) e^{i\mathbf{k}\cdot\mathbf{x}} \\ &= \int \frac{d^3\mathbf{k}}{(2\pi)^{3/2}} \left[\hat{a}_{\mathbf{k}} f_k(\eta) e^{i\mathbf{k}\cdot\mathbf{x}} + \hat{a}_{\mathbf{k}}^\dagger f_k^*(\eta) e^{-i\mathbf{k}\cdot\mathbf{x}} \right], \end{aligned} \quad (8)$$

where the annihilation and creation operators $\hat{a}_{\mathbf{k}}$ and $\hat{a}_{\mathbf{k}}^\dagger$ satisfy the standard commutation relations, viz.

$$[\hat{a}_{\mathbf{k}}, \hat{a}_{\mathbf{k}'}] = [\hat{a}_{\mathbf{k}}^\dagger, \hat{a}_{\mathbf{k}'}^\dagger] = 0, \quad [\hat{a}_{\mathbf{k}}, \hat{a}_{\mathbf{k}'}^\dagger] = \delta^{(3)}(\mathbf{k} - \mathbf{k}'). \quad (9)$$

To obtain the solutions for the mode functions f_k , one often works with the associated Mukhanov-Sasaki variable v_k —defined as $v_k = z f_k$ —which satisfies the differential equation

$$v_k'' + \left(k^2 - \frac{z''}{z} \right) v_k = 0. \quad (10)$$

The scalar power spectrum is defined as

$$\mathcal{P}_s(k) = \frac{k^3}{2\pi^2} |f_k|^2 = \frac{k^3}{2\pi^2} \frac{|v_k|^2}{z^2}, \quad (11)$$

where the quantities f_k , v_k and z are to be evaluated at late times close to the end of inflation.

¹ We should clarify a point on nomenclature here. We find that scenarios with constant p are also referred to as constant roll inflation [64, 65]. We shall be focusing on scenarios wherein $p > 3$. In such cases, the first slow roll parameter decreases so rapidly that the amplitude of the curvature perturbations grows indefinitely at late times. Hence, we believe it is more apt to refer to these scenarios as ultra slow roll inflation.

Let us first consider the case of ultra slow inflation wherein $p = 6$. In such a case, we have $\epsilon_1 = \epsilon_{1i} (a_i/a)^6$ and $z = \sqrt{2\epsilon_{1i}} M_{\text{Pl}} a_i^3 (H_1 \eta)^2$, so that $z''/z = 2/\eta^2$. As this is similar to the case of pure de Sitter, the solution to the mode function f_k , which satisfies the standard Bunch-Davies condition in the domain wherein $k \gg \sqrt{z''/z}$ [which corresponds to the sub-Hubble limit $k/(aH) \simeq (-k\eta) \gg 1$], can be immediately obtained to be

$$\begin{aligned} f_k(\eta) &= \frac{1}{\sqrt{2\epsilon_{1i}} M_{\text{Pl}} a_i^3 H_1^2 \eta^2} \frac{1}{\sqrt{2k}} \left(1 - \frac{i}{k\eta}\right) e^{-ik\eta} \\ &= \frac{-H_1}{\sqrt{4k\epsilon_{1i}} M_{\text{Pl}}} \left(\frac{\eta_i^3}{\eta^2}\right) \left(1 - \frac{i}{k\eta}\right) e^{-ik\eta}. \end{aligned} \quad (12)$$

The resulting scalar power spectrum, evaluated at a late time, say, η_e , corresponding to the end of inflation, turns out to be

$$\mathcal{P}_s(k) = \frac{H_1^2}{8\pi^2 M_{\text{Pl}}^2 \epsilon_{1i}} \left[\frac{a(\eta_e)}{a_i}\right]^6 = \frac{H_1^2}{8\pi^2 M_{\text{Pl}}^2 \epsilon_{1i}} \left(\frac{\eta_i}{\eta_e}\right)^6. \quad (13)$$

There are two points concerning this scalar power spectrum that need to be emphasized. The first point is the fact the spectrum is independent of k , i.e. it is scale invariant. The second point is that, in contrast to slow roll inflation, the spectrum does not approach a constant value at late times [i.e. when $k \ll \sqrt{z''/z}$, which is equivalent to the super-Hubble limit $k/(aH) \simeq (-k\eta) \ll 1$]. In fact, the power spectrum grows as a^6 at late times. This can be attributed to the fact that the mode function f_k grows as a^3 in the super-Hubble limit. Such a growth is a well known feature in the ultra slow roll inflationary scenarios [57, 58].

Let us now turn to the case of $p = 4$. When $p = 4$, we have $\epsilon_1 = \epsilon_{1i} (a_i/a)^4$ and $z = \sqrt{2\epsilon_{1i}} M_{\text{Pl}} (-H_1 \eta)$ so that $z''/z = 0$. It should be evident that the solution to the mode function f_k which satisfies the Bunch-Davies initial condition is given by

$$\begin{aligned} f_k(\eta) &= \frac{1}{\sqrt{2\epsilon_{1i}} a_i^2 M_{\text{Pl}} (-H_1 \eta)} \frac{1}{\sqrt{2k}} e^{-ik\eta} \\ &= \frac{-H_1}{\sqrt{4k\epsilon_{1i}} M_{\text{Pl}}} \left(\frac{\eta_i^2}{\eta}\right) e^{-ik\eta}. \end{aligned} \quad (14)$$

The scalar power spectrum evaluated at the end of inflation (corresponding to the conformal time η_e) can be expressed as

$$\begin{aligned} \mathcal{P}_s(k) &= \frac{H_1^2}{8\pi^2 M_{\text{Pl}}^2 \epsilon_{1i}} \left(\frac{k}{a_i H_1}\right)^2 \left[\frac{a(\eta_e)}{a_i}\right]^2 \\ &= \frac{H_1^2}{8\pi^2 M_{\text{Pl}}^2 \epsilon_{1i}} \left(\frac{\eta_i}{\eta_e}\right)^2 (k\eta_i)^2. \end{aligned} \quad (15)$$

As in the case of $p = 6$, the mode function f_k and the scalar power spectrum $\mathcal{P}_s(k)$ grow indefinitely at late times. Moreover, note that, the above spectrum has a strong blue tilt, as it behaves as k^2 .

C. Mode functions describing the electromagnetic field and power spectra

In a FLRW universe, the conformal invariance of the standard electromagnetic action dilutes the amplitude of the cosmological magnetic fields as $B \propto 1/a^2$. The dilution is, in particular, considerable during the inflationary epoch. Therefore, to generate magnetic fields during inflation that are consistent with the current observations (say, $10^{-16} < B_0 < 10^{-9}$ G), the conformal invariance of the electromagnetic action must be broken. This is usually achieved by introducing a function in the action which couples the electromagnetic field to the inflaton, say, ϕ . The electromagnetic action that is often considered in such a case has the form (see, for example, Refs. [5, 37])

$$S[A^\mu] = -\frac{1}{16\pi} \int d^4x \sqrt{-g} J^2(\phi) F_{\mu\nu} F^{\mu\nu}, \quad (16)$$

where $J(\phi)$ denotes the non-conformal coupling function and the field tensor $F_{\mu\nu}$ is expressed in terms of the vector potential A_μ as $F_{\mu\nu} = (\partial_\mu A_\nu - \partial_\nu A_\mu)$.

We can arrive at the equation of motion governing the vector potential A_μ by varying the above action. In what follows, we shall choose to work in the Coulomb gauge wherein $A_0 = 0$ and $(g^{ij} \partial_i A_j) = 0$. Let \bar{A}_k denote the Fourier mode functions associated with the vector potential A_i . We find that the mode functions \bar{A}_k satisfy the following differential equation (see, for example, Refs. [5, 37]):

$$\bar{A}_k'' + 2 \frac{J'}{J} \bar{A}_k' + k^2 \bar{A}_k = 0. \quad (17)$$

If we write $\bar{A}_k = \mathcal{A}_k/J$, then this differential equation simplifies to the form

$$\mathcal{A}_k'' + \left(k^2 - \frac{J''}{J}\right) \mathcal{A}_k = 0. \quad (18)$$

For each comoving wave vector \mathbf{k} , we can define the polarization vector $\epsilon_\lambda^{\mathbf{k}}$, where $\lambda = \{1, 2\}$ represents the two states of polarization of the electromagnetic field. The polarization vector satisfies the condition $\mathbf{k} \cdot \epsilon_\lambda^{\mathbf{k}} = 0$. Moreover, the components $\epsilon_{\lambda i}^{\mathbf{k}}$ of the polarization vector satisfy the relation

$$\sum_{\lambda=1}^2 \epsilon_{\lambda i}^{\mathbf{k}} \epsilon_{\lambda j}^{\mathbf{k}} = \delta_{ij} - \frac{k_i k_j}{k^2}, \quad (19)$$

where k_i denotes the components of the wave vector \mathbf{k} . On quantization, the vector potential A_i can be decomposed in terms of the mode functions \bar{A}_k as follows:

$$\begin{aligned} \hat{A}_i(\eta, \mathbf{x}) &= \sqrt{4\pi} \int \frac{d^3\mathbf{k}}{(2\pi)^{3/2}} \sum_{\lambda=1}^2 \epsilon_{\lambda i}^{\mathbf{k}} \left[\hat{b}_{\mathbf{k}}^\lambda \bar{A}_k(\eta) e^{i\mathbf{k}\cdot\mathbf{x}} \right. \\ &\quad \left. + \hat{b}_{\mathbf{k}}^{\lambda\dagger} \bar{A}_k^*(\eta) e^{-i\mathbf{k}\cdot\mathbf{x}} \right]. \end{aligned} \quad (20)$$

The creation and annihilation operators $\hat{b}_{\mathbf{k}}^\lambda$ and $\hat{b}_{\mathbf{k}}^{\lambda\dagger}$ satisfy the following commutation relations:

$$[\hat{b}_{\mathbf{k}}^\lambda, \hat{b}_{\mathbf{k}'}^{\lambda'}] = [\hat{b}_{\mathbf{k}}^{\lambda\dagger}, \hat{b}_{\mathbf{k}'}^{\lambda'\dagger}] = 0, \quad [\hat{b}_{\mathbf{k}}^\lambda, \hat{b}_{\mathbf{k}'}^{\lambda'\dagger}] = \delta^{(3)}(\mathbf{k} - \mathbf{k}') \delta^{\lambda\lambda'}. \quad (21)$$

The energy densities associated with the electric and magnetic fields, say, ρ_B and ρ_E , are given by

$$\rho_B = \frac{J^2}{16\pi a^4} \delta^{im} \delta^{jn} F_{ij} F_{mn}, \quad (22a)$$

$$\rho_E = \frac{J^2}{8\pi a^4} \delta^{ij} A'_i A'_j. \quad (22b)$$

Let $\hat{\rho}_B$ and $\hat{\rho}_E$ denote the operators associated with the corresponding energy densities. The power spectra of the magnetic and electric fields, say, $\mathcal{P}_B(k)$ and $\mathcal{P}_E(k)$, are defined as [5, 37]

$$\mathcal{P}_B(k) = \frac{d\langle 0|\hat{\rho}_B|0\rangle}{d\ln k}, \quad \mathcal{P}_E(k) = \frac{d\langle 0|\hat{\rho}_E|0\rangle}{d\ln k}, \quad (23)$$

where $|0\rangle$ denotes the vacuum state annihilated by the annihilation operator $\hat{b}_{\mathbf{k}}^\lambda$, i.e. $\hat{b}_{\mathbf{k}}^\lambda|0\rangle = 0$ for all \mathbf{k} and λ . On utilizing the decomposition of the vector potential in Eq. (20), the power spectra $\mathcal{P}_B(k)$ and $\mathcal{P}_E(k)$ can be expressed in terms of the mode functions \bar{A}_k and their scaled forms \mathcal{A}_k as follows [5, 37]:

$$\mathcal{P}_B(k) = \frac{k^5}{2\pi^2} \frac{J^2}{a^4} |\bar{A}_k|^2 = \frac{k^5}{2\pi^2 a^4} |\mathcal{A}_k|^2, \quad (24a)$$

$$\mathcal{P}_E(k) = \frac{k^3}{2\pi^2} \frac{J^2}{a^4} |\bar{A}'_k|^2 = \frac{k^3}{2\pi^2 a^4} \left| \mathcal{A}'_k - \frac{J'}{J} \mathcal{A}_k \right|^2. \quad (24b)$$

Let us now discuss the spectra of electric and magnetic fields that arise in the standard scenarios. Evidently, the spectra will depend on the choice of the coupling function $J(\phi)$. Often, the coupling function is assumed to be a simple function of the scale factor as follows [5, 37]:

$$J(\eta) = \left[\frac{a(\eta)}{a(\eta_e)} \right]^{\bar{n}}, \quad (25)$$

where η_e is the conformal time at the end of inflation and \bar{n} is a number. Note that the overall coefficient has been chosen so that the coupling function J reduces to unity at the end of inflation (i.e. at η_e). In situations wherein the scale factor can be expressed in the de Sitter form, the coupling function is given by

$$J(\eta) = \left(\frac{\eta}{\eta_e} \right)^{-\bar{n}}. \quad (26)$$

For such a choice of the coupling function, the solution to Eq. (18) that satisfies the Bunch-Davies initial conditions in the domain wherein $k \gg \sqrt{J''/J}$ [which corresponds to the sub-Hubble limit $(-k\eta) \ll 1$ for the J we are working with] can be expressed as

$$\mathcal{A}_k(\eta) = \sqrt{-\frac{\pi\eta}{4}} e^{i(\bar{n}+1)\pi/2} H_\nu^{(1)}(-k\eta), \quad (27)$$

where $\nu = \bar{n} + (1/2)$, and $H_\nu^{(1)}(z)$ denotes the Hankel function of the first kind.

The spectra of the electromagnetic fields can be evaluated at late times when $k \ll \sqrt{J''/J}$, i.e. in the super-Hubble limit wherein $(-k\eta) \ll 1$. Upon substituting the mode functions given in Eq. (27) in the expressions in Eqs. (24) and considering the super-Hubble limit, the spectra of the magnetic and electric fields $\mathcal{P}_B(k)$ and $\mathcal{P}_E(k)$ can be obtained to be [5, 37]

$$\mathcal{P}_B(k) = \frac{H_1^4}{8\pi} \mathcal{F}(m) (-k\eta_e)^{2m+6}, \quad (28a)$$

$$\mathcal{P}_E(k) = \frac{H_1^4}{8\pi} \mathcal{G}(m) (-k\eta_e)^{2m+4}. \quad (28b)$$

The quantities $\mathcal{F}(m)$ and $\mathcal{G}(m)$ are given by

$$\mathcal{F}(m) = \frac{1}{2^{2m+1} \cos^2(m\pi) \Gamma^2(m+3/2)}, \quad (29a)$$

$$\mathcal{G}(m) = \frac{1}{2^{2m-1} \cos^2(m\pi) \Gamma^2(m+1/2)}, \quad (29b)$$

with

$$m = \begin{cases} \bar{n}, & \text{for } \bar{n} < -\frac{1}{2}, \\ -\bar{n} - 1, & \text{for } \bar{n} > -\frac{1}{2}, \end{cases} \quad (30)$$

in the case of $\mathcal{P}_B(k)$, and with

$$m = \begin{cases} \bar{n}, & \text{for } \bar{n} < \frac{1}{2}, \\ 1 - \bar{n}, & \text{for } \bar{n} > \frac{1}{2}, \end{cases} \quad (31)$$

in the case of $\mathcal{P}_E(k)$. Note that the spectral indices for the magnetic and electric fields, say, n_B and n_E , can be written as

$$n_B = \begin{cases} 2\bar{n} + 6, & \text{for } \bar{n} < -\frac{1}{2}, \\ 4 - 2\bar{n}, & \text{for } \bar{n} > -\frac{1}{2}, \end{cases} \quad (32)$$

and

$$n_E = \begin{cases} 2\bar{n} + 4, & \text{for } \bar{n} < \frac{1}{2}, \\ 6 - 2\bar{n}, & \text{for } \bar{n} > \frac{1}{2}. \end{cases} \quad (33)$$

There are a few points that we need to clarify regarding the results that we have arrived at above. To begin with, note that, we obtain a scale invariant spectrum for the magnetic field when $\bar{n} = 2$ and when $\bar{n} = -3$. However, when $\bar{n} = -3$, the spectrum of the electric field behaves as $\mathcal{P}_E(k) \propto (-k\eta_e)^{-2}$, which grows indefinitely at late times. In other words, the energy density in the electric field becomes large leading to significant backreaction on the background (in this regard, see, for instance, Refs. [40, 55]). Therefore, when we require a scale invariant spectrum for the magnetic field, we shall focus on the $\bar{n} = 2$ case. Secondly, recall that the original non-conformal coupling function J depends on ϕ [cf. Eq. (16)]. Whereas, our choices for J in Eqs. (25) and (26) depend on the scale factor and conformal time. Such a

behavior for $J(\eta)$ is achievable in most models of inflation that permit slow roll [38, 39, 76]. However, there exist situations, in particular, when an inflationary potential permits a period of ultra slow roll, wherein a behavior such as $J \propto a^2 \propto \eta^{-2}$ may not be achievable (for discussions in this context, see Ref. [55]). To circumvent such challenges, either, one has to consider inflation involving more than one field (for a discussion on this point, see Ref. [56]) or, as we shall discuss in the following section, consider more non-trivial forms for the coupling functions involving the kinetic energy of the inflaton.

III. CONSTRUCTION OF THE NON-CONFORMAL COUPLING FUNCTION IN PURE ULTRA SLOW ROLL INFLATION

We had pointed out earlier that a phase of ultra slow roll inflation is achieved as the inflaton approaches a point of inflection in the potential. Hence, during the period of ultra slow roll, the velocity of the inflaton drops rapidly and the field hardly evolves. In such situations, the non-conformal coupling function $J(\phi)$ becomes nearly a constant and, as a result, the quantity J''/J turns out to be very small. This behavior effectively restores the conformal invariance of the electromagnetic action [55]. One finds that the electromagnetic spectra behave as k^4 over wave numbers that leave the Hubble radius after the onset of ultra slow roll. Moreover, the amplitude of the magnetic fields on large scales (which leave the Hubble radius during the initial period of slow roll, prior to the transition to the phase of ultra slow roll), is considerably suppressed.

To circumvent this difficulty, we shall now construct a non-conformal coupling function J that involves the time derivative of the inflaton. Such a coupling function proves to be particularly effective in the scenario of *pure* ultra slow roll inflation that is of interest in this work. Recall that, in ultra slow roll inflation, the first slow roll parameter ϵ_1 behaves as in Eq. (6), where $p > 3$. It should then be clear that, if we have a coupling function that behaves as $\epsilon_1^{n/2}$, for a suitable choice of the index n , we will be able to achieve the behavior of, say, $J \propto \eta^{-2}$, as is required to lead to a scale invariant spectrum for the magnetic field.

Since $\epsilon_1 = \dot{\phi}^2/(2H^2 M_{\text{Pl}}^2)$ and the Hubble parameter H is nearly a constant in ultra slow roll inflation, we can assume that the non-conformal coupling function J depends on the scalar quantity $X = -(1/2)\partial_\sigma\phi\partial^\sigma\phi = \dot{\phi}^2/2$. Therefore, we can rewrite the action governing the electromagnetic field in the following form²:

$$S[A^\mu] = -\frac{1}{16\pi} \int d^4x \sqrt{-g} J^2(X) F_{\mu\nu} F^{\mu\nu}. \quad (34)$$

² We should mention that a different action involving derivatives of the inflaton has been considered earlier [77].

We shall assume that the coupling function is given by

$$J(X) = J_0 \left(-\frac{\partial_\sigma\phi\partial^\sigma\phi}{2} \right)^{n/2}, \quad (35)$$

where J_0 is a constant which we shall choose so that J reduces to unity at the end of inflation. It should be evident that, since the non-conformal coupling function $J(X)$ depends only on time, the electromagnetic field described by the action in Eq. (34) can be treated in the same manner as in the case of the field described by the earlier action in Eq. (16). For instance, if we work in the Coulomb gauge, the Fourier modes A_k of the vector potential A_i will continue to satisfy the same equation of motion, viz. Eq. (17). Also, on quantization, we can elevate the vector potential A_i to the operator \hat{A}_i as in Eq. (20). Note that, in the ultra slow roll inflationary scenarios of interest, we can write the coupling function in Eq. (35) as

$$J(\eta) = J_0 [H_1^2 M_{\text{Pl}}^2 \epsilon_1(\eta)]^{n/2}, \quad (36)$$

and we shall choose $J_0 = [H_1^2 M_{\text{Pl}}^2 \epsilon_1(\eta_e)]^{-n/2}$ so that $J(\eta_e) = 1$. Therefore, the coupling function can be simply written as follows:

$$J(\eta) = \left[\frac{\epsilon_1(\eta)}{\epsilon_1(\eta_e)} \right]^{n/2}. \quad (37)$$

On varying the action in Eq. (34) with respect to the metric tensor, we obtain the stress-energy tensor for the electromagnetic field to be

$$\begin{aligned} T_{\alpha\beta} = & -\frac{J_0^2}{16\pi} g_{\alpha\beta} (-\partial_\sigma\phi\partial^\sigma\phi)^n F_{\mu\nu} F^{\mu\nu} \\ & -\frac{J_0^2 n}{8\pi} (-\partial_\sigma\phi\partial^\sigma\phi)^{n-1} (\partial_\alpha\phi\partial_\beta\phi) F_{\mu\nu} F^{\mu\nu} \\ & +\frac{J_0^2}{4\pi} (\partial_\sigma\phi\partial^\sigma\phi)^n g^{\mu\nu} F_{\alpha\mu} F_{\beta\nu}. \end{aligned} \quad (38)$$

We find that, in the background described by the FLRW line-element described by Eq. (1), the energy density of the electromagnetic field, viz. $\rho_{\text{EM}} = -T_t^t$, can be expressed as

$$\rho_{\text{EM}} = (1 + 2n) \rho_{\text{E}} + (1 - 2n) \rho_{\text{B}}, \quad (39)$$

where ρ_{B} and ρ_{E} are the energy densities we had introduced earlier in Eqs. (22). Since the factors $(1 - 2n)$ and $(1 + 2n)$ in the above expression are numbers of the order of unity, we shall continue to define the power spectra $\mathcal{P}_{\text{B}}(k)$ and $\mathcal{P}_{\text{E}}(k)$ of the magnetic and electric fields as we had done in Eq. (23). Clearly, in such a case, the power spectra $\mathcal{P}_{\text{B}}(k)$ and $\mathcal{P}_{\text{E}}(k)$ will be given by Eqs. (24), with $J(\eta)$ given by Eq. (37). We shall evaluate the power spectra at the end of inflation (i.e. at η_e). As n can be positive or negative, a concern may arise if the expectation value of the total energy density—i.e. $\langle \hat{\rho}_{\text{EM}} \rangle$, with ρ_{EM} given by Eq. (39)—is positive definite. We shall discuss this issue

in App. A. We shall show that, in all the scenarios we consider, the quantity $\langle \hat{\rho}_{\text{EM}} \rangle$ always remains positive.

Recall that, in ultra slow roll inflation, the first slow roll parameter behaves as $\epsilon_1 \propto \eta^p$ [cf. Eq. (6)]. Also, as we discussed in Sec. II C, in order to obtain a scale invariant spectrum for the magnetic field, we need the coupling function to behave as $J \propto \eta^{-2}$. It should then be clear from Eq. (37) that we can obtain a scale invariant spectrum for the magnetic field if we choose $n_p = -4$. In such a case, we find that the mode function \bar{A}_k and the scaled variable \mathcal{A}_k are given by

$$\mathcal{A}_k(\eta) = -\frac{1}{\sqrt{2k^5\eta^2}} (3 + 3ik\eta - k^2\eta^2) e^{-ik\eta}, \quad (40a)$$

$$\bar{A}_k(\eta) = -\frac{1}{\sqrt{2k^5\eta_e^2}} (3 + 3ik\eta - k^2\eta^2) e^{-ik\eta}. \quad (40b)$$

On using these solutions in Eqs. (24), we obtain the power spectra of the magnetic and electric fields to be

$$\mathcal{P}_B(k) \simeq \frac{9H_1^4}{4\pi^2}, \quad \mathcal{P}_E(k) \simeq \frac{H_1^4}{4\pi^2} (-k\eta_e)^2. \quad (41)$$

Note that, while the power spectrum of the magnetic field $\mathcal{P}_B(k)$ is scale invariant, the spectrum of the electric field behaves as $\mathcal{P}_E(k) \propto k^2$. However, since η_e is small, on large scales, the strength of $\mathcal{P}_E(k)$ is significantly suppressed when compared to that of $\mathcal{P}_B(k)$.

IV. CUBIC ORDER ACTION AND THE CROSS-CORRELATION BETWEEN CURVATURE PERTURBATIONS AND MAGNETIC FIELDS

It is well known that, if the primordial perturbations were Gaussian, all their statistical properties would be contained in the two-point functions. In such a case, while the higher-order even-point functions can be expressed in terms of the two-point functions, the higher-order odd-point functions would vanish. However, if the perturbations were not Gaussian, the odd-point functions can, in general, be expected to be non-zero. This carries importance because, in many situations, the non-Gaussianities can significantly alter the predictions of the cosmological observables (in this context, see, for example, Refs. [51, 78–87]). Evidently, these arguments also apply to primordial magnetic fields. At the level of the two-point functions, one finds that many models of inflation generate magnetic fields with scale invariant spectra. So, to distinguish between the various models from the perspective of electromagnetic fields, it is not adequate to study only the two-point functions. We need to evaluate the higher-order correlations, such as the three-point functions. The three-point cross-correlation between the scalar perturbations and the magnetic fields has been studied extensively in the case of slow roll inflation [88–95]. Our aim in this

work will be to evaluate the three-point cross-correlation in the scenario of *pure* ultra slow roll inflation. We shall focus on particular cases that exhibit certain behaviour for the power spectra of the scalar perturbations and the electromagnetic fields. Specifically, we shall investigate the behavior of the cross-correlation in the squeezed limit wherein the wave number of the scalar perturbation is much smaller than the wave numbers of the two electromagnetic modes.

A. Action at the cubic order

As is often done, we shall compute the three-point function using the standard methods of perturbative quantum field theory (for calculations involving scalars and tensors, see, for example, Refs. [96–100], and for discussions involving magnetic fields, see Refs. [89–95, 101]). Our first task is to obtain the interaction Hamiltonian at the cubic order that governs the cross-correlation of interest. We shall start with the action in Eq. (34), take into account the scalar perturbations in the spatially flat, FLRW line-element, and arrive at the cubic order action involving the curvature perturbations and the electromagnetic fields. We shall make use of the Arnowitt–Deser–Misner (ADM) formalism to obtain the action [102]. Recall that, in the ADM formalism, the line-element associated with a generic spacetime is described in terms of the lapse function N , the shift vector N^i and the spatial metric g_{ij} as follows:

$$ds^2 = -N^2 (dx^0)^2 + g_{ij} (N^i dx^0 + dx^i) (N^j dx^0 + dx^j). \quad (42)$$

Note that the metric elements g_{00} and g_{0i} associated with this line-element are given by

$$g_{00} = -N^2 + g_{ij} N^i N^j, \quad g_{0i} = g_{ij} N^j. \quad (43)$$

We shall work in the gauge wherein the perturbations in the inflaton are absent. In such a case, to account for the scalar perturbations, we can write the spatial element g_{ij} of the spatially flat, FLRW line-element as follows:

$$g_{ij} = \delta_{ij} a^2 e^{2\mathcal{R}}, \quad (44)$$

where, as we have mentioned, \mathcal{R} denotes the curvature perturbation. The lapse and the shift functions N and N_i can be determined from the constraint equations at the first order. If we work with the conformal time coordinate and write $N = a(1 + N_1)$ and $g_{ij} N^j = a^2 \partial_i \chi$, where N_1 and χ are the inhomogeneous terms, we find that the constraint equations determine N_1 and χ to be

$$N_1 = \frac{\mathcal{R}'}{aH}, \quad \chi = -\frac{\mathcal{R}}{aH} + \epsilon_1 \nabla^{-2} \mathcal{R}'. \quad (45)$$

On substituting the above components of the metric tensor in the action in Eq. (34), we find that the action *up to*

the cubic order involving the curvature perturbation \mathcal{R} and the electromagnetic vector potential A_i can be expressed as

$$S[\mathcal{R}, A_i] = -\frac{1}{16\pi} \int d\eta \int d^3\mathbf{x} J^2(\eta) \left\{ -2 \left[1 + \mathcal{R} - (1 + 2n) \frac{\mathcal{R}'}{aH} \right] \delta^{ij} A'_i A'_j \right. \\ \left. + 4 \delta^{il} \delta^{jm} \partial_i \chi A'_j F_{lm} + \left[1 - \mathcal{R} + (1 - 2n) \frac{\mathcal{R}'}{aH} \right] \delta^{im} \delta^{jn} F_{ij} F_{mn} \right\}, \quad (46)$$

where, in the cases of our interest, the non-conformal coupling function $J(\eta)$ is given by Eq. (37). To calculate the three-point cross-correlation, we shall require the cubic order Hamiltonian associated with the above action. From the action, we obtain the momentum conjugate to the vector potential A_i , say, π_i , to be

$$\pi_i = -\frac{a^2(\eta)}{4\pi} J^2(\eta) \left\{ - \left[1 + \mathcal{R} - (1 + 2n) \frac{\mathcal{R}'}{aH} \right] A'_i + \left[1 + \mathcal{R} - (1 + 2n) \frac{\mathcal{R}'}{aH} \right] \delta^{jl} \partial_j \chi F_{li} \right\}. \quad (47)$$

We can make use of this conjugate momentum to construct the Hamiltonian and identify the cubic order terms as the interaction Hamiltonian H_{int} . We obtain the interaction Hamiltonian to be

$$H_{\text{int}} = -\frac{1}{16\pi} \int d^3\mathbf{x} J^2(\eta) \left\{ 2 \left[\mathcal{R} - (1 + 2n) \frac{\mathcal{R}'}{aH} \right] \delta^{ij} A'_i A'_j - 4 \delta^{il} \delta^{jm} \partial_i \chi A'_j F_{lm} \right. \\ \left. + \left[\mathcal{R} - (1 - 2n) \frac{\mathcal{R}'}{aH} \right] \delta^{im} \delta^{jn} F_{ij} F_{mn} \right\}. \quad (48)$$

There are two clarifying remarks that we wish to make regarding the interaction Hamiltonian H_{int} we have obtained. Firstly, note that, in the above Hamiltonian, if we ignore the terms containing n within the curly brackets, it reduces to the standard form associated with the original action in Eq. (16) involving $J(\phi)$ (in this regard, see, for example, Refs. [90, 91]). Secondly, as with any action at the cubic order, the interaction Hamiltonian proves to be negative of the corresponding cubic order Lagrangian.

B. Three-point cross-correlation

We shall now turn to the computation of the three-point cross-correlation using the interaction Hamiltonian in Eq. (48). In real space, the cross-correlation between the curvature perturbation and magnetic fields is defined as

$$\langle \hat{\mathcal{R}}(\eta, \mathbf{x}) \hat{B}^i(\eta, \mathbf{x}) \hat{B}_i(\eta, \mathbf{x}) \rangle = \int \frac{d^3\mathbf{k}_1}{(2\pi)^{3/2}} \int \frac{d^3\mathbf{k}_2}{(2\pi)^{3/2}} \int \frac{d^3\mathbf{k}_3}{(2\pi)^{3/2}} \langle \hat{\mathcal{R}}_{\mathbf{k}_1}(\eta) \hat{B}_{\mathbf{k}_2}^i(\eta) \hat{B}_{\mathbf{k}_3}(\eta) \rangle e^{i(\mathbf{k}_1 + \mathbf{k}_2 + \mathbf{k}_3) \cdot \mathbf{x}}, \quad (49)$$

where the components B_i of the magnetic fields are related to those of the vector potential A_i through the relation

$$B_i = \frac{1}{a} \epsilon_{ijl} \partial_j A_l. \quad (50)$$

We had mentioned above that we shall make use of perturbative quantum field theory to arrive at the three-point cross-correlation. According to quantum field theory, given the cubic order Hamiltonian H_{int} , the three-point cross-correlation in Fourier space, evaluated at the conformal time η_e corresponding to the end of inflation, is given by

$$\langle \hat{\mathcal{R}}_{\mathbf{k}_1}(\eta_e) \hat{B}_{\mathbf{k}_2}^i(\eta_e) \hat{B}_{\mathbf{k}_3}(\eta_e) \rangle = -i \int_{\eta_i}^{\eta_e} d\eta \langle [\hat{\mathcal{R}}_{\mathbf{k}_1}(\eta_e) \hat{B}_{\mathbf{k}_2}^i(\eta_e) \hat{B}_{\mathbf{k}_3}(\eta_e), \hat{H}_{\text{int}}(\eta)] \rangle, \quad (51)$$

where \hat{H}_{int} is the operator associated with the interaction Hamiltonian in Eq. (48), and η_i denotes the time when the initial conditions are imposed on the perturbations. Moreover, the square brackets denote the commutator between the operators denoting modes of the curvature perturbation, the magnetic field, and the Hamiltonian operator.

To describe the cross-correlation between the modes of the curvature perturbation and the magnetic field, we shall

introduce the function $\mathcal{B}(\mathbf{k}_1, \mathbf{k}_2, \mathbf{k}_3)$ that is defined through the relation³

$$\langle \hat{\mathcal{R}}_{\mathbf{k}_1}(\eta_e) \hat{B}_{\mathbf{k}_2}^i(\eta_e) \hat{B}_{i\mathbf{k}_3}(\eta_e) \rangle = \frac{4\pi}{(2\pi)^{3/2}} \mathcal{B}(\mathbf{k}_1, \mathbf{k}_2, \mathbf{k}_3) \delta^{(3)}(\mathbf{k}_1 + \mathbf{k}_2 + \mathbf{k}_3). \quad (52)$$

On making use of the expression in Eq. (51), the interaction Hamiltonian in Eq. (48), the definition of the three-point function in Eq. (52) and, finally, Wick's theorem, we find that the function $\mathcal{B}(\mathbf{k}_1, \mathbf{k}_2, \mathbf{k}_3)$ can be written as follows [89–92, 101, 103]:

$$\mathcal{B}(\mathbf{k}_1, \mathbf{k}_2, \mathbf{k}_3) = \sum_{C=1}^6 \mathcal{B}_C(\mathbf{k}_1, \mathbf{k}_2, \mathbf{k}_3) = \frac{1}{a^4(\eta_e)} \sum_{C=1}^6 [f_{\mathbf{k}_1}(\eta_e) \bar{A}_{\mathbf{k}_2}(\eta_e) \bar{A}_{\mathbf{k}_3}(\eta_e) \mathcal{G}_C(\mathbf{k}_1, \mathbf{k}_2, \mathbf{k}_3) + \text{complex conjugate}], \quad (53)$$

where the quantities $\mathcal{G}_C(\mathbf{k}_1, \mathbf{k}_2, \mathbf{k}_3)$, with $C = \{1, 6\}$, are described by the integrals

$$\mathcal{G}_1(\mathbf{k}_1, \mathbf{k}_2, \mathbf{k}_3) = -2i(\mathbf{k}_2 \cdot \mathbf{k}_3) \int_{\eta_i}^{\eta_e} d\eta J^2(\eta) f_{\mathbf{k}_1}^*(\eta) \bar{A}'_{\mathbf{k}_2}(\eta) \bar{A}'_{\mathbf{k}_3}(\eta), \quad (54a)$$

$$\mathcal{G}_2(\mathbf{k}_1, \mathbf{k}_2, \mathbf{k}_3) = 2i(1+2n)(\mathbf{k}_2 \cdot \mathbf{k}_3) \int_{\eta_i}^{\eta_e} \frac{d\eta}{aH} J^2(\eta) f_{\mathbf{k}_1}^*(\eta) \bar{A}'_{\mathbf{k}_2}(\eta) \bar{A}'_{\mathbf{k}_3}(\eta), \quad (54b)$$

$$\mathcal{G}_3(\mathbf{k}_1, \mathbf{k}_2, \mathbf{k}_3) = i[(\mathbf{k}_1 \cdot \mathbf{k}_2)k_3^2 + (\mathbf{k}_1 \cdot \mathbf{k}_3)(\mathbf{k}_2 \cdot \mathbf{k}_3)] \int_{\eta_i}^{\eta_e} \frac{d\eta}{aH} J^2(\eta) f_{\mathbf{k}_1}^*(\eta) \bar{A}'_{\mathbf{k}_2}(\eta) \bar{A}'_{\mathbf{k}_3}(\eta) + \mathbf{k}_2 \leftrightarrow \mathbf{k}_3, \quad (54c)$$

$$\mathcal{G}_4(\mathbf{k}_1, \mathbf{k}_2, \mathbf{k}_3) = \frac{i}{k_1^2} [(\mathbf{k}_1 \cdot \mathbf{k}_2)k_3^2 + (\mathbf{k}_1 \cdot \mathbf{k}_3)(\mathbf{k}_2 \cdot \mathbf{k}_3)] \int_{\eta_i}^{\eta_e} d\eta J^2(\eta) \epsilon_1(\eta) f_{\mathbf{k}_1}^*(\eta) \bar{A}'_{\mathbf{k}_2}(\eta) \bar{A}'_{\mathbf{k}_3}(\eta) + \mathbf{k}_2 \leftrightarrow \mathbf{k}_3, \quad (54d)$$

$$\mathcal{G}_5(\mathbf{k}_1, \mathbf{k}_2, \mathbf{k}_3) = i[k_2^2 k_3^2 + (\mathbf{k}_2 \cdot \mathbf{k}_3)^2] \int_{\eta_i}^{\eta_e} d\eta J^2(\eta) f_{\mathbf{k}_1}^*(\eta) \bar{A}'_{\mathbf{k}_2}(\eta) \bar{A}'_{\mathbf{k}_3}(\eta), \quad (54e)$$

$$\mathcal{G}_6(\mathbf{k}_1, \mathbf{k}_2, \mathbf{k}_3) = -i(1-2n)[k_2^2 k_3^2 + (\mathbf{k}_2 \cdot \mathbf{k}_3)^2] \int_{\eta_i}^{\eta_e} \frac{d\eta}{aH} J^2(\eta) f_{\mathbf{k}_1}^*(\eta) \bar{A}'_{\mathbf{k}_2}(\eta) \bar{A}'_{\mathbf{k}_3}(\eta). \quad (54f)$$

We should mention that these six integrals are exact expressions and they have been arrived at without making any approximations.

Using the solutions for f_k and \bar{A}_k in the pure ultra slow roll scenarios that we discussed in the previous two sections, we can compute the integrals $\mathcal{G}_C(\mathbf{k}_1, \mathbf{k}_2, \mathbf{k}_3)$. In App. B we have presented the explicit forms of $\mathcal{G}_C(\mathbf{k}_1, \mathbf{k}_2, \mathbf{k}_3)$ for two cases of p and suitable choices for n that lead to scale invariant spectra of the magnetic fields. Using the expressions for $\mathcal{G}_C(\mathbf{k}_1, \mathbf{k}_2, \mathbf{k}_3)$, we can compute the different contributions to the cross-correlation $\mathcal{B}(\mathbf{k}_1, \mathbf{k}_2, \mathbf{k}_3)$. We shall discuss these results in the next section.

C. Non-Gaussianity parameter

In addition to the cross-correlation $\mathcal{B}(\mathbf{k}_1, \mathbf{k}_2, \mathbf{k}_3)$, we shall compute the associated non-Gaussianity parameter $b_{\text{NL}}(\mathbf{k}_1, \mathbf{k}_2, \mathbf{k}_3)$. The parameter is usually expressed as a dimensionless quantity involving the ratio of the three-point cross-correlation and the scalar power spectrum and the power spectrum of the magnetic field [89–92, 101]. The parameter reflects the amplitude and shape of the three-point function and it helps in distinguishing among various models of inflation as well as between inflationary and alternative scenarios of the early universe which lead to the same power spectra.

To arrive at the form of the non-Gaussianity parameter $b_{\text{NL}}(\mathbf{k}_1, \mathbf{k}_2, \mathbf{k}_3)$, let us express the magnetic field in terms of the Gaussian components and the parameter as

³ In the definition in Eq. (52) of the three-point function, we have introduced an additional factor of (4π) in comparison to the earlier works in the literature (in this context, see Refs. [89–92, 103]). Note that our electromagnetic actions in Eqs. (16) and (34) contain an additional factor of $1/(4\pi)$ in comparison to the action in the previous works. In order to ensure that the expression for the power spectrum of the magnetic field remains the same, we had included an overall factor of $\sqrt{4\pi}$ in the expression for the vector potential A_i in Eq. (20). However, such a definition for A_i introduces another factor of (4π) when we evaluate the quantity on the right hand side of Eq. (51), which is not present if we instead follow the normalization conventions used in the aforementioned works. Therefore, in order to ensure that the quantity $\mathcal{B}(\mathbf{k}_1, \mathbf{k}_2, \mathbf{k}_3)$ remains the same across the different conventions, we have introduced the factor of (4π) in Eq. (52).

follows:

$$\hat{B}_{i\mathbf{k}}(\eta) = \hat{B}_{i\mathbf{k}}^{\text{G}}(\eta) + \frac{1}{(2\pi)^{3/2}} \int d^3\mathbf{p} \hat{\mathcal{R}}_{\mathbf{p}}^{\text{G}}(\eta) \hat{B}_{i\mathbf{k}-\mathbf{p}}^{\text{G}}(\eta) \times b_{\text{NL}}(\mathbf{p}, \mathbf{k}, \mathbf{k}-\mathbf{p}), \quad (55)$$

where $\hat{B}_{i\mathbf{k}}^{\text{G}}$ and $\hat{\mathcal{R}}_{\mathbf{k}}^{\text{G}}$ represent the Gaussian parts of the Fourier modes of the magnetic field and the curvature perturbation, respectively. If we compute the cross-correlation $\mathcal{B}(\mathbf{k}_1, \mathbf{k}_2, \mathbf{k}_3)$ using the above expression and utilize Wick's theorem which applies to the Gaussian components, we obtain the expression for $b_{\text{NL}}(\mathbf{k}_1, \mathbf{k}_2, \mathbf{k}_3)$ to be

$$b_{\text{NL}}(\mathbf{k}_1, \mathbf{k}_2, \mathbf{k}_3) = \frac{1}{8\pi^4} J^2(\eta) \times \frac{k_1^3 k_2^3 k_3^3 \mathcal{B}(\mathbf{k}_1, \mathbf{k}_2, \mathbf{k}_3)}{\mathcal{P}_s(k_1) [k_3^3 \mathcal{P}_B(k_2) + k_2^3 \mathcal{P}_B(k_3)]}, \quad (56)$$

where, recall that, $\mathcal{P}_s(k)$ and $\mathcal{P}_B(k)$ represent the scalar power spectrum and the power spectrum of the magnetic field.

An important property of the three-point functions is their behavior in the so-called squeezed limit wherein one of the three wavelengths is much longer than the other two. In the squeezed limit, under certain conditions, it has been shown that the three-point functions can be expressed entirely in terms of the two-point functions. This is often referred to as the consistency relation [47, 91, 92, 95, 96, 101, 104–112]. Such a consistency condition primarily arises because of the reason that, in the scenarios involving slow roll, the amplitude of the long-wavelength perturbation freezes in the super-Hubble regime. As far as the three-point cross-correlation of our interest is concerned, such a consistency relation can be expected to arise when one considers the mode associated with the curvature perturbation to be the long wavelength mode. Indeed, such a relation has been established in slow roll inflation (in this context, see Refs. [91, 92]). In the following sections, apart from computing the three-point cross-correlation and the associated non-Gaussianity parameter, we shall also explicitly examine if the standard consistency condition is valid in the scenarios involving ultra slow roll inflation.

V. CALCULATION OF THE CROSS-CORRELATION AND ASSOCIATED NON-GAUSSIANITY PARAMETER

We shall now evaluate the three-point cross-correlation $\mathcal{B}(\mathbf{k}_1, \mathbf{k}_2, \mathbf{k}_3)$ and the associated non-Gaussianity parameter $b_{\text{NL}}(\mathbf{k}_1, \mathbf{k}_2, \mathbf{k}_3)$ in the ultra slow roll inflationary scenarios we considered earlier. Before discussing the amplitude and shape of the non-Gaussianity parameter, we shall clarify a few points regarding the scalar power spectra and the power spectra of the magnetic field, and arrive at suitable values of the parameters involved.

A. Power spectra

We shall begin by fixing the Hubble parameter during inflation H_1 using the condition that the scalar power at the pivot scale of $k_* = 0.05 \text{ Mpc}^{-1}$ is normalized by the CMB observations to be $\mathcal{P}_s(k_*) \simeq 2 \times 10^{-9}$. Fixing H_1 in such a manner is not straightforward and is dependent on the ultra slow scenario that we are considering. Recall that, in the ultra slow roll scenarios with $p = 6$ and $p = 4$, the scalar power spectrum is given by [cf. Eqs. (13) and (15)]

$$\mathcal{P}_s(k) \simeq \begin{cases} \frac{H_1^2}{8\pi^2 \epsilon_{1i} M_{\text{Pl}}^2} \left(\frac{\eta_i}{\eta_e}\right)^6, & \text{for } p = 6, \\ \frac{H_1^2}{8\pi^2 \epsilon_{1i} M_{\text{Pl}}^2} \left(\frac{\eta_i}{\eta_e}\right)^2 (k \eta_i)^2, & \text{for } p = 4. \end{cases} \quad (57)$$

Demanding $\mathcal{P}_s(k_*) \simeq 2 \times 10^{-9}$ implies that the Hubble parameter is to be set to

$$H_1 \simeq \begin{cases} 4\pi 10^{-9/2} \sqrt{\epsilon_{1i}} \left(\frac{\eta_e}{\eta_i}\right)^3 M_{\text{Pl}}, & \text{for } p = 6, \\ 4\pi 10^{-9/2} \sqrt{\epsilon_{1i}} \left(\frac{\eta_e}{\eta_i}\right) \frac{1}{|k_* \eta_i|} M_{\text{Pl}}, & \text{for } p = 4. \end{cases} \quad (58)$$

Let us then turn to the power spectrum of the tensor perturbations. Recall that the equation of motion that governs the tensor perturbations is solely dictated by the behavior of the scale factor $a(\eta)$. Also, note that the scale factor during ultra slow roll inflation can be approximated well by the de Sitter form as $a(\eta) = -1/(H_1 \eta)$. Hence, the spectrum of tensor perturbations in the ultra slow roll scenarios of interest (for $p = 6$ as well as 4) is given by the standard form in slow roll inflation, viz.

$$\mathcal{P}_T(k) \simeq \frac{2H_1^2}{\pi^2 M_{\text{Pl}}^2}. \quad (59)$$

Next, we set $\eta_i = -10^6 \text{ Mpc}$ so that the largest observable scale of $k \simeq 10^{-4} \text{ Mpc}^{-1}$ is sufficiently deep inside the Hubble radius at the beginning of inflation. We shall assume that inflation lasts for about 65 e-folds. In such a case, $\eta_e = -10^{-19} \text{ Mpc}$, which determines the smallest scale that exits the Hubble radius during inflation to be $k \simeq 10^{19} \text{ Mpc}^{-1}$. Lastly, we choose $\epsilon_{1i} = 10^{-3}$ as an indicative value. It is related to the tensor-to-scalar ratio at the pivot scale of k_* , which in these cases turns out to be

$$r = \begin{cases} 16 \epsilon_{1i} \left(\frac{\eta_e}{\eta_i}\right)^6, & \text{for } p = 6, \\ 16 \epsilon_{1i} \left(\frac{\eta_e}{\eta_i}\right)^2 \left(\frac{1}{k_* \eta_i}\right)^2, & \text{for } p = 4. \end{cases} \quad (60)$$

We should caution the readers about a few points concerning the behavior of these spectra and the related choices for the parameters. The first issue is regarding the shape of the spectra. The case of $p = 4$ leads to a scalar power spectrum with a strong scale-dependence of $\mathcal{P}_s(k) \propto k^2$ and it is clearly at odds with the CMB data. So, this case is being examined solely for gaining a

theoretical understanding of the effects of ultra slow roll inflation. The case of $p = 6$ performs better in terms of the shape of the scalar power spectrum. In this case, the scalar power spectrum $\mathcal{P}_s(k)$ is strictly scale invariant. Although, such a spectrum is disfavored by the CMB data, the value of p (or, equivalently, the second slow roll parameter ϵ_2) can be tuned slightly to achieve the required spectral index of $n_s \simeq 0.965$.

Another outcome of these choices is that the Hubble parameter H_1 and, hence, the tensor-to-scalar ratio r are highly suppressed (in both the cases of $p = 6$ and 4) by factors of the ratio η_e/η_i . Note that $\eta_e/\eta_i \simeq 10^{-25}$. Therefore, for instance, when $p = 6$, we have $H_1/M_{\text{Pl}} \simeq 10^{-80}$, which corresponds to an energy scale that is smaller than the scale of big bang nucleosynthesis! So, with any value of ϵ_{1i} less than unity, we have a highly suppressed tensor power and hence r in the ultra slow roll scenarios.

This brings us to yet another issue that we encounter. Recall that the amplitude of the scale invariant spectrum of the magnetic field is given by $\mathcal{P}_B(k) \simeq 9 H_1^4/(4\pi^2)$ [cf. Eq. (41)]. Since H_1 is very small, the strengths of the generated magnetic fields is proportionately suppressed in ultra slow roll inflation. If we focus specifically on the case of $p = 6$, we find that the spectrum of the magnetic field can be expressed as

$$\mathcal{P}_B(k) \simeq \frac{9 H_1^4}{4\pi^2} \simeq 9(4\pi\epsilon_{1i})^2 \left(\frac{\eta_e}{\eta_i}\right)^{12} \mathcal{P}_S(k_*) M_{\text{Pl}}^4. \quad (61)$$

In contrast, the typical value of $\mathcal{P}_B(k)$ obtained in slow roll inflation with a coupling function behaving as $J(\eta) \propto \eta^{-2}$ would be

$$\mathcal{P}_B(k) \simeq \frac{9 H_1^4}{4\pi^2} \simeq 9(4\pi\epsilon_{1i})^2 \mathcal{P}_S(k_*) M_{\text{Pl}}^4. \quad (62)$$

Clearly, the amplitude of $\mathcal{P}_B(k)$ in ultra slow roll inflation is suppressed by a factor of $(\eta_e/\eta_i)^{12} \sim 10^{-300}$. Such a small value of $\mathcal{P}_B(k)$ will not be sufficient to serve as seeds for magnetic fields with the strengths observed in the inter-galactic medium today. Despite these shortcomings of the scenario of pure ultra slow roll, we pursue the analysis with the aim of eventually utilizing the coupling function that we have constructed in a realistic model of inflation with a brief epoch of ultra slow roll. We shall now proceed with these values of the parameters to calculate and examine the amplitude and shape of the non-Gaussianity parameter $b_{\text{NL}}(\mathbf{k}_1, \mathbf{k}_2, \mathbf{k}_3)$.

B. Amplitude and shape of the non-Gaussianity parameter

We shall evaluate the cross-correlation $\mathcal{B}(\mathbf{k}_1, \mathbf{k}_2, \mathbf{k}_3)$ between the curvature perturbation and the magnetic fields in ultra slow roll inflationary scenarios with $p = 6$ and 4. We shall consider $J(\eta)$ as given by Eq. (37) and focus on the case of $n p = -4$ which leads to a scale invariant spectrum for the magnetic field. It should be clear from Eqs. (53) and (54) that the calculation of the three-point cross-correlation first requires the evaluation of the integrals $\mathcal{G}_C(\mathbf{k}_1, \mathbf{k}_2, \mathbf{k}_3)$. With the background quantities and the Fourier mode functions f_k as well as \bar{A}_k of the curvature perturbation and the electromagnetic vector potential at hand, we can carry out the integrals $\mathcal{G}_C(\mathbf{k}_1, \mathbf{k}_2, \mathbf{k}_3)$. The integrals are easy to compute. But, since the expressions describing the integrals prove to be lengthy, we have listed the results for these integrals in the different cases in App. B. In what follows, we shall list the results for the various contributions to $\mathcal{B}(\mathbf{k}_1, \mathbf{k}_2, \mathbf{k}_3)$ and discuss the structure of the corresponding non-Gaussianity parameter $b_{\text{NL}}(\mathbf{k}_1, \mathbf{k}_2, \mathbf{k}_3)$.

1. Case of $p = 6$

When $p = 6$ and $n = -2/3$ so that $n p = -4$, we can use the forms of the slow roll parameter $\epsilon_1(\eta)$ and the coupling function $J(\eta)$ [cf. Eqs. (6) and (37)] as well as the corresponding Fourier mode functions $f_k(\eta)$ and $\bar{A}_k(\eta)$ describing the curvature perturbation and the electromagnetic vector potential [cf. Eqs. (12) and (40b)] to evaluate the integrals $\mathcal{G}_C(\mathbf{k}_1, \mathbf{k}_2, \mathbf{k}_3)$. Once we have evaluated the quantities $\mathcal{G}_C(\mathbf{k}_1, \mathbf{k}_2, \mathbf{k}_3)$, we can substitute them and the mode functions $f_k(\eta)$ and $\bar{A}_k(\eta)$ in Eq. (53) to arrive at the different contributions $\mathcal{B}_C(\mathbf{k}_1, \mathbf{k}_2, \mathbf{k}_3)$ to the three-point cross-correlation of interest. We find that the leading terms (as $\eta_e \rightarrow 0$) in the different contributions are given by

$$\mathcal{B}_1(\mathbf{k}_1, \mathbf{k}_2, \mathbf{k}_3) = -\frac{3 H_1^6 \eta_i^2}{32 M_{\text{Pl}}^2 k_1^3 k_2^3 k_3^3 \epsilon_{1i}} \left(\frac{\eta_i}{\eta_e}\right)^4 (k_1^2 - k_2^2 - k_3^2) [3k_1^3 + 4(k_2^3 + k_3^3)], \quad (63a)$$

$$\mathcal{B}_2(\mathbf{k}_1, \mathbf{k}_2, \mathbf{k}_3) = \frac{3 H_1^6 \eta_i^2}{32 M_{\text{Pl}}^2 k_1^3 k_2^3 k_3^3 \epsilon_{1i}} \left(\frac{\eta_i}{\eta_e}\right)^4 (k_1^2 - k_2^2 - k_3^2) [k_1^3 - 4(k_2^3 + k_3^3)], \quad (63b)$$

$$\mathcal{B}_3(\mathbf{k}_1, \mathbf{k}_2, \mathbf{k}_3) = \frac{9 H_1^6 \eta_i^2}{128 M_{\text{Pl}}^2 \epsilon_{1i} k_1^3 k_2^3 k_3^5} \left(\frac{\eta_i}{\eta_e}\right)^4 [(k_1^2 - k_2^2)^2 + 2(k_1^2 + k_2^2)k_3^2 - 3k_3^4] (3k_1^3 + 4k_2^3) + \mathbf{k}_2 \leftrightarrow \mathbf{k}_3, \quad (63c)$$

$$\mathcal{B}_4(\mathbf{k}_1, \mathbf{k}_2, \mathbf{k}_3) = \frac{81 \pi H_1^6}{64 M_{\text{Pl}}^2 k_1^5 k_2^3 k_3^5 \eta_e^3} [(k_1 - k_2)^2 + 2(k_1^2 + k_2^2)k_3^2 - 3k_3^4] + \mathbf{k}_2 \leftrightarrow \mathbf{k}_3, \quad (63d)$$

$$\mathcal{B}_5(\mathbf{k}_1, \mathbf{k}_2, \mathbf{k}_3) = \frac{9 H_1^6}{64 M_{\text{Pl}}^2 k_2^5 k_3^5 \epsilon_{1i}} \left(\frac{\eta_i}{\eta_e} \right)^6 [k_1^4 + k_2^4 - 2 k_1^2 (k_2^2 + k_3^2) + 6 k_2^2 k_3^2 + k_3^4], \quad (63e)$$

$$\mathcal{B}_6(\mathbf{k}_1, \mathbf{k}_2, \mathbf{k}_3) = \frac{63 H_1^6}{64 M_{\text{Pl}}^2 k_2^5 k_3^5 \epsilon_{1i}} \left(\frac{\eta_i}{\eta_e} \right)^6 [k_1^4 + k_2^4 - 2 k_1^2 (k_2^2 + k_3^2) + 6 k_2^2 k_3^2 + k_3^4]. \quad (63f)$$

Clearly, among the different contributions, it is the fifth and the sixth terms, viz. $\mathcal{B}_5(\mathbf{k}_1, \mathbf{k}_2, \mathbf{k}_3)$ and $\mathcal{B}_6(\mathbf{k}_1, \mathbf{k}_2, \mathbf{k}_3)$, that dominate. Note that these contributions behave as $(\eta_i/\eta_e)^6$, just as the scalar power spectrum $\mathcal{P}_s(k)$ does when $p = 6$ [cf. Eq. (13)]. Since the magnetic power spectrum $\mathcal{P}_B(k)$ is a constant [cf. Eq. (41)], we find that resulting non-Gaussianity parameter $b_{\text{NL}}(\mathbf{k}_1, \mathbf{k}_2, \mathbf{k}_3)$ turns out to be independent of η_e and is given by

$$b_{\text{NL}}(\mathbf{k}_1, \mathbf{k}_2, \mathbf{k}_3) = \frac{k_1^3}{2 k_2^2 k_3^2 (k_2^3 + k_3^3)} [k_1^4 + k_2^4 - 2 k_1^2 (k_2^2 + k_3^2) + 6 k_2^2 k_3^2 + k_3^4]. \quad (64)$$

Let us now discuss the amplitude of the non-Gaussianity parameter $b_{\text{NL}}(\mathbf{k}_1, \mathbf{k}_2, \mathbf{k}_3)$ for various configurations of the wave vectors. In the equilateral limit wherein $k_1 = k_2 = k_3 = k$, we find that the parameter $b_{\text{NL}}(k)$ given by Eq. (64) above turns out to be independent of the wave number and is given by

$$b_{\text{NL}}^{\text{eq}}(k) \simeq \frac{5}{4}. \quad (65)$$

In the flattened limit with the configuration $k_1 = 2 k_2 = 2 k_3 = 2 k$, we find that

$$b_{\text{NL}}^{\text{fl}}(k) \simeq 16. \quad (66)$$

Finally, in the squeezed limit wherein $k_1 \rightarrow 0$ and $k_2 = k_3 = k$, we obtain that

$$b_{\text{NL}}^{\text{sq}}(k_1, k) \simeq 2 \left(\frac{k_1}{k} \right)^3 \left\{ 1 - \frac{1}{2} \left(\frac{k_1}{k} \right)^2 + \mathcal{O} \left[\left(\frac{k_1}{k} \right)^4 \right] \right\} + \mathcal{O}(k^2 \eta_e^2). \quad (67)$$

Evidently, in the squeezed limit, the leading contribution to $b_{\text{NL}}(k_1, k)$ is proportional to k_1^3 , which vanishes. However, we find that there is a subleading contribution to the non-Gaussianity parameter which is proportional to $(k^2 \eta_e^2)$. But, since $(k \eta_e)$ is very small, this contribution is also rather small. For instance, if we choose $k = k_* \simeq 5 \times 10^{-2} \text{ Mpc}^{-1}$, then, for the choice of $\eta_e = -10^{-19} \text{ Mpc}$, we obtain that $b_{\text{NL}}^{\text{sq}} \simeq \mathcal{O}(10^{-42})$. We shall comment further about the behavior of the non-Gaussianity parameter in the squeezed limit when we discuss the consistency relation in the subsequent subsection.

To understand the complete structure of the non-Gaussianity parameter $b_{\text{NL}}(\mathbf{k}_1, \mathbf{k}_2, \mathbf{k}_3)$, in Fig. 1, we have illustrated it for all possible configurations of wave vectors. We have presented the behavior of $b_{\text{NL}}(\mathbf{k}_1, \mathbf{k}_2, \mathbf{k}_3)$ for $p = 6$ as a density plot in the two-dimensional plane of k_1/k_3 - k_2/k_3 , with $k_3 = k_*$. Note that this plot is obtained using the complete expression for $b_{\text{NL}}(\mathbf{k}_1, \mathbf{k}_2, \mathbf{k}_3)$ as given in Eq. (64). We find that $b_{\text{NL}}(\mathbf{k}_1, \mathbf{k}_2, \mathbf{k}_3)$ peaks in the region around the flattened limit (i.e. when $k_1 = k_3 + k_2$) where it attains the maximum value of 16. It steadily falls towards zero in the squeezed limit, i.e. when $k_1 \rightarrow 0$ and $k_2 = k_3$. These behavior are indeed expected from the results in the flattened and squeezed limits we have already arrived at in Eqs. (66) and (67).

2. Case of $p = 4$

When $p = 4$, as in the previous case, we can utilize the behavior of $\epsilon_1(\eta)$ and $J(\eta)$ as well as the associated solutions for the Fourier mode functions $f_k(\eta)$ and $\bar{A}_k(\eta)$ [as given in Eqs. (14)] and (40b)] to evaluate the integrals $\mathcal{G}_C(\mathbf{k}_1, \mathbf{k}_2, \mathbf{k}_3)$ and arrive at the different contributions $\mathcal{B}_C(\mathbf{k}_1, \mathbf{k}_2, \mathbf{k}_3)$ to the cross-correlation. Again, we choose the value of n such that $n p = -4$, which leads to $n = -1$ in this case. We obtain the different contributions $\mathcal{B}_C(\mathbf{k}_1, \mathbf{k}_2, \mathbf{k}_3)$ to be

$$\mathcal{B}_1(\mathbf{k}_1, \mathbf{k}_2, \mathbf{k}_3) = -\frac{9 H_1^6 \eta_i^2}{16 M_{\text{Pl}}^2 k_2^3 k_3^3 \epsilon_{1i}} \left(\frac{\eta_i}{\eta_e} \right)^2 (k_1^2 - k_2^2 - k_3^2), \quad (68a)$$

$$\mathcal{B}_2(\mathbf{k}_1, \mathbf{k}_2, \mathbf{k}_3) = \frac{9 H_1^6 \eta_i^2}{16 M_{\text{Pl}}^2 k_2^3 k_3^3 \epsilon_{1i}} \left(\frac{\eta_i}{\eta_e} \right)^2 (k_1^2 - k_2^2 - k_3^2), \quad (68b)$$

$$\mathcal{B}_3(\mathbf{k}_1, \mathbf{k}_2, \mathbf{k}_3) = \frac{27 H_1^6 \eta_i^2}{64 M_{\text{Pl}}^2 k_2^3 k_3^3 \epsilon_{1i}} \left(\frac{\eta_i}{\eta_e} \right)^2 [(k_1^2 - k_2^2)^2 + 2(k_1^2 + k_2^2)k_3^2 - 3k_3^4] + \mathbf{k}_2 \leftrightarrow \mathbf{k}_3, \quad (68c)$$

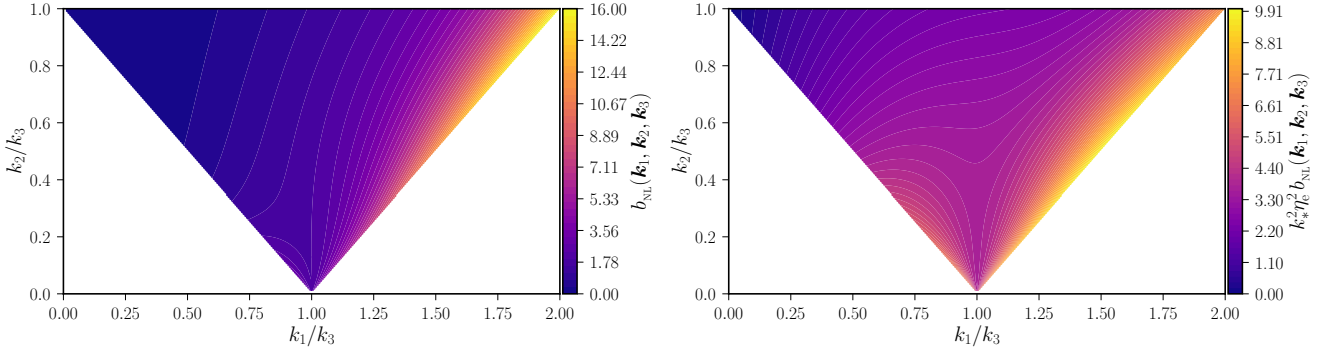


FIG. 1. We present the complete structure of the non-Gaussianity parameter $b_{\text{NL}}(\mathbf{k}_1, \mathbf{k}_2, \mathbf{k}_3)$ as density plots in the plane of k_1/k_3 - k_2/k_3 for the cases of $p = 6$ (on the left) and $p = 4$ (on the right). Note that, in the case of $p = 4$, due to the behavior $b_{\text{NL}}(\mathbf{k}_1, \mathbf{k}_2, \mathbf{k}_3) \propto \eta_e^{-2}$, we have plotted the dimensionless combination $k_3^2 \eta_e^2 b_{\text{NL}}(\mathbf{k}_1, \mathbf{k}_2, \mathbf{k}_3)$. We have set $\epsilon_{1i} = 10^{-3}$, $\eta_i = -10^6$ Mpc and $\eta_e = -10^{-19}$ Mpc, as discussed in the text. Further, we have set $k_3 = k_* = 5 \times 10^{-2} \text{Mpc}^{-1}$ to arrive at the plots. We should highlight that, in both the cases of $p = 6$ and $p = 4$, the magnitude of $b_{\text{NL}}(\mathbf{k}_1, \mathbf{k}_2, \mathbf{k}_3)$ spans over a wide range of values between the flattened limit (on the top right corners of the density plots wherein $k_1 = 2k_2 = 2k_3$) and the squeezed limit (on the top left corners wherein $k_1 \rightarrow 0$ and $k_2 \simeq k_3$).

$$\mathcal{B}_4(\mathbf{k}_1, \mathbf{k}_2, \mathbf{k}_3) = \frac{27 \pi H_1^6}{64 M_{\text{Pl}}^2 k_1^3 k_2^3 k_3^5 \eta_e} [(k_1^2 - k_2^2)^2 + 2(k_1^2 + k_2^2)k_3^2 - 3k_3^4] + \mathbf{k}_2 \leftrightarrow \mathbf{k}_3, \quad (68d)$$

$$\mathcal{B}_5(\mathbf{k}_1, \mathbf{k}_2, \mathbf{k}_3) = \frac{27 H_1^6}{128 M_{\text{Pl}}^2 k_2^5 k_3^5 \epsilon_{1i}} \left(\frac{\eta_i}{\eta_e} \right)^4 [k_1^4 + k_2^4 - 2k_1^2(k_2^2 + k_3^2) + 6k_2^2 k_3^2 + k_3^4], \quad (68e)$$

$$\mathcal{B}_6(\mathbf{k}_1, \mathbf{k}_2, \mathbf{k}_3) = \frac{243 H_1^6}{128 M_{\text{Pl}}^2 k_2^5 k_3^5 \epsilon_{1i}} \left(\frac{\eta_i}{\eta_e} \right)^4 [k_1^4 + k_2^4 - 2k_1^2(k_2^2 + k_3^2) + 6k_2^2 k_3^2 + k_3^4]. \quad (68f)$$

Note that, as in the case of $p = 6$, it is the fifth and the sixth terms, viz. $\mathcal{B}_5(\mathbf{k}_1, \mathbf{k}_2, \mathbf{k}_3)$ and $\mathcal{B}_6(\mathbf{k}_1, \mathbf{k}_2, \mathbf{k}_3)$, that dominate the contributions. If we take into account these contributions, we find that the corresponding non-Gaussianity parameter $b_{\text{NL}}(\mathbf{k}_1, \mathbf{k}_2, \mathbf{k}_3)$ turns out to be

$$b_{\text{NL}}(\mathbf{k}_1, \mathbf{k}_2, \mathbf{k}_3) = \frac{15 k_1}{16 k_2^2 k_3^2 (k_2^3 + k_3^3) \eta_e^2} [k_1^4 + k_2^4 - 2k_1^2(k_2^2 + k_3^2) + 6k_2^2 k_3^2 + k_3^4]. \quad (69)$$

A notable feature of the non-Gaussianity parameter $b_{\text{NL}}(\mathbf{k}_1, \mathbf{k}_2, \mathbf{k}_3)$ in this case is the dependence on η_e as η_e^{-2} . This is a large factor and it affects the amplitude of the parameter across all configurations. On inspecting the various limits, we find that, in the equilateral limit (i.e. when $k_1 = k_2 = k_3 = k$), the expression Eq. (69) above simplifies to

$$b_{\text{NL}}^{\text{eq}}(k) \simeq \frac{75}{32 k^2 \eta_e^2}. \quad (70)$$

For the value of the parameter $\eta_e = -10^{-19}$ Mpc as fixed earlier, at $k_* = 5 \times 10^{-2} \text{Mpc}^{-1}$, we obtain that $b_{\text{NL}}^{\text{eq}} \simeq 9.375 \times 10^{40}$. In the flattened limit (i.e. when $k_1 = 2k_2 = 2k_3 = 2k$), we get

$$b_{\text{NL}}^{\text{fl}}(k) \simeq \frac{15}{2 k^2 \eta_e^2}, \quad (71)$$

which at k_* turns out to be $b_{\text{NL}}^{\text{fl}} \simeq 3 \times 10^{41}$. In the squeezed

limit (i.e. when $k_1 \rightarrow 0$ and $k_2 = k_3 = k$), we obtain that

$$b_{\text{NL}}^{\text{sq}}(k_1, k) \simeq \frac{15}{4 k^2 \eta_e^2} \left(\frac{k_1}{k} \right) \left\{ 1 - \frac{1}{2} \left(\frac{k_1}{k} \right)^2 + \mathcal{O} \left[\left(\frac{k_1}{k} \right)^4 \right] \right\} + \mathcal{O}(k \eta_e). \quad (72)$$

We can see that, as $k_1 \rightarrow 0$ in the squeezed limit, the leading order contribution to $b_{\text{NL}}(k_1, k)$ is proportional to k_1 and hence vanishes. However, there is a subleading contribution that is proportional to $(k \eta_e)$, which becomes relevant only in the squeezed limit. For the pivot scale of $k_* = 5 \times 10^{-2} \text{Mpc}^{-1}$ and, for our choice of $\eta_e = -10^{-19}$ Mpc, the contribution proves to be very small. In fact, we find that $b_{\text{NL}}^{\text{sq}} \simeq \mathcal{O}(10^{-21})$. We shall discuss the corresponding implications for the consistency relation governing the three-point function in the next subsection.

As in the earlier case, when $p = 4$, we have presented the complete structure of the parameter $b_{\text{NL}}(\mathbf{k}_1, \mathbf{k}_2, \mathbf{k}_3)$ as a density plot in Fig. 1. Note that this plot is ob-

tained using the expression for $b_{\text{NL}}(\mathbf{k}_1, \mathbf{k}_2, \mathbf{k}_3)$ as given in Eq. (69). We find that $b_{\text{NL}}(\mathbf{k}_1, \mathbf{k}_2, \mathbf{k}_3)$ peaks in the region around the flattened limit where $k_1 = k_2 + k_3$, as in the $p = 6$ case. In the case of $p = 4$, the parameter reaches extremely large values across all configurations because of the general behavior of $b_{\text{NL}}(\mathbf{k}_1, \mathbf{k}_2, \mathbf{k}_3)$ as η_e^{-2} , as we mentioned earlier. Hence, we have plotted the combination $k_3^2 \eta_e^2 b_{\text{NL}}(\mathbf{k}_1, \mathbf{k}_2, \mathbf{k}_3)$ to better understand its structure for different configurations of wave numbers. This combination reaches values as large as 7.5 in the flattened limit and it vanishes in the squeezed limit. These behavior are as expected from the different limits we already arrived at in Eqs. (71) and (72). Such large values for the non-Gaussianity parameter $b_{\text{NL}}(\mathbf{k}_1, \mathbf{k}_2, \mathbf{k}_3)$ may lead to strong non-Gaussian corrections to the power spectrum of the magnetic field $\mathcal{P}_{\text{B}}(k)$. We shall relegate the examination of such a possibility to App. C, wherein we shall discuss some interesting results.

C. Consistency relation

The behavior of the three-point cross-correlation $\mathcal{B}(\mathbf{k}_1, \mathbf{k}_2, \mathbf{k}_3)$ in the squeezed limit (i.e. when $k_1 \rightarrow 0$ and $\mathbf{k}_2 = -\mathbf{k}_3$) is expected to be governed by the consistency relation that we had mentioned earlier. This relation allows us to express the non-Gaussianity parameter $b_{\text{NL}}(\mathbf{k}_1, \mathbf{k}_2, \mathbf{k}_3)$ in the squeezed limit in terms of the spectral index of the magnetic power spectrum, say, $n_{\text{B}}(k)$, which is, in general, defined as $n_{\text{B}}(k) = d \ln \mathcal{P}_{\text{B}}(k) / d \ln k$. In the case of slow roll inflation, the consistency relation is obtained to be [92, 103]

$$b_{\text{NL}}^{\text{cr}} = \frac{4 - n_{\text{B}}}{2}. \quad (73)$$

This relation has been verified by explicit calculations in the case of slow roll inflation [in this context, see Eqs. (D3) and (D4) as well as the associated discussion in App. D]. Both the ultra slow roll scenarios described so far have the coupling function behaving as $J \propto \eta^{-2}$, thereby leading to a scale invariant power spectrum for the magnetic field (i.e. $n_{\text{B}} = 0$). As should be evident from Eqs. (67), (72) and (73), the consistency relation is violated in these cases. Besides the ultra slow roll scenarios discussed thus far which lead to a scale invariant $\mathcal{P}_{\text{B}}(k)$, in App. D, we have considered another scenario where $\mathcal{P}_{\text{B}}(k)$ is not scale invariant, but has a spectral index of $n_{\text{B}} = 2$. In this case, according to the consistency relation, we should obtain that $b_{\text{NL}}^{\text{cr}} = 1$. However, we instead obtain $b_{\text{NL}}^{\text{sq}} = 0$ [cf. Eq. (D2c)], which also violates the consistency relation.

In Tab. I, we have listed the values of $b_{\text{NL}}^{\text{sq}}$ obtained in the different scenarios we have considered. We have also listed the values of $b_{\text{NL}}^{\text{cr}}$ that we are expected to obtain. From the table, we can clearly see that, while the consistency relation is satisfied in slow roll inflation, for a similar behavior of $J(\eta)$, it is violated in ultra slow roll inflation. The standard consistency relations arise in situations wherein the amplitude of the long wave length

α	n_{B}	$b_{\text{NL}}^{\text{sq}}$ in slow roll	$b_{\text{NL}}^{\text{sq}}$ in ultra slow roll	$b_{\text{NL}}^{\text{cr}}$
2	0	2	0	2
1	2	1	0	1

TABLE I. We have listed the values of the non-Gaussianity parameter $b_{\text{NL}}(\mathbf{k}_1, \mathbf{k}_2, \mathbf{k}_3)$ obtained in the squeezed limit in the various scenarios of interest. We have assumed that $J \propto \eta^{-\alpha}$ in arriving at these results. We have also listed the corresponding values of b_{NL} that we expect to obtain from the consistency condition given in Eq. (73). It is clear that, while the consistency relation is satisfied in slow roll inflation, it is violated in the ultra slow roll scenarios.

mode freezes [96, 97, 113, 114]. In slow roll inflation, we find that the consistency relation in Eq. (73) is satisfied by the non-Gaussianity parameter $b_{\text{NL}}(\mathbf{k}_1, \mathbf{k}_2, \mathbf{k}_3)$ in the squeezed limit since, in such situations, the amplitude of the curvature perturbation goes to a constant value on super-Hubble scales. In contrast, in pure ultra slow roll inflation, the amplitude of the curvature perturbations grows indefinitely at late times. The violation of the consistency relation [as given by Eq. (73)] that we encounter in the ultra slow roll scenarios can be ascribed to the growth in the amplitude of the curvature perturbations on super-Hubble scales. One expects the consistency relation in Eq. (73) to be modified in such situations (for related discussions in the case of the scalar bispectrum, see Refs. [59–61]). It will be interesting to derive a generic consistency condition that governs the non-Gaussianity parameter $b_{\text{NL}}(\mathbf{k}_1, \mathbf{k}_2, \mathbf{k}_3)$ in the squeezed limit, including non-trivial evolution of the long wave length curvature perturbation. However, such a derivation is beyond the scope of this work and we hope to address the problem in the future.

VI. CONCLUSIONS

Models of inflation that permit a brief phase of ultra slow roll have attracted attention in the recent literature because they lead to scalar power spectra with higher amplitudes over small scales. Such scalar spectra with enhanced power on small scales can produce copious amounts of primordial black holes and also induce secondary gravitational waves of considerable strengths. In this work, we investigated the generation of magnetic fields in scenarios of ultra slow roll inflation. It has been pointed out that there arise certain challenges in generating magnetic fields with nearly scale invariant spectra and of observed strengths in single field inflationary models that permit a short period of ultra slow roll (see Ref. [55]; in this context, also see Ref. [56]). To circumvent such a challenge, rather than considering the electromagnetic action involving the popular non-conformal coupling function $J(\phi)$ [cf. Eq. (16)], we worked with an action involving a function of the form $J(X)$ [cf. Eq. (34)]. We focused on *pure* ultra slow roll scenarios. In other words,

we assumed that the phase of ultra slow roll lasts throughout the entire duration of inflation. While such scenarios do not seem viable when compared with the observations, we considered these scenarios to gain a better understanding of the effects of ultra slow roll on the two-point and three-point functions involving the magnetic fields. We worked with a non-conformal coupling function $J(X)$ which turned out to be proportional to a power of the first slow roll parameter in the ultra slow roll scenarios. We find that, for suitable choices of parameters describing the non-conformal coupling function and the inflationary scenario, we can obtain scale invariant spectra for the magnetic fields. However, we should mention that, for our choice of parameters, the coupling function does indeed exhibit the strong coupling problem during early times. One of the ways to ameliorate this issue is to consider a ‘sawtooth’ coupling (for detailed discussions, see, for example, Refs. [103, 115, 116]). We are currently studying implementations of such coupling functions in ultra slow roll scenarios.

For our choice of $J(X)$, we also calculated the three-point cross-correlation $\mathcal{B}(\mathbf{k}_1, \mathbf{k}_2, \mathbf{k}_3)$ involving the curvature perturbation and the magnetic fields in the ultra slow roll scenarios. We examined the amplitude and shape of the associated non-Gaussianity parameter $b_{\text{NL}}(\mathbf{k}_1, \mathbf{k}_2, \mathbf{k}_3)$ arising in a few different cases. When compared to slow roll inflation, we find that the values of the non-Gaussianity parameter in the ultra slow roll scenario of $p = 6$, with $n = -2/3$, leading to scale invariant scalar and magnetic power spectra, are considerably smaller [cf. Eqs. (65), (66) and (67)]. However, we find that the values of $b_{\text{NL}}(\mathbf{k}_1, \mathbf{k}_2, \mathbf{k}_3)$ can vary significantly depending on the ultra slow roll scenario and the value of n being considered. For example, in the case wherein we obtain a scale invariant spectrum for the magnetic field and a blue scalar power spectrum [with $\mathcal{P}_s(k) \propto k^2$], we obtain very large values for the non-Gaussianity parameter (see right panel of Fig. 1 and the accompanying discussion). In contrast, in the ultra slow roll scenario which leads to a scale invariant scalar power spectrum and a blue magnetic power spectrum [with $\mathcal{P}_B(k) \propto k^2$], we obtain very small values for the non-Gaussianity parameter (see App. D). Specifically, we had examined the validity of the consistency condition that the three-point function of interest is expected to satisfy in the squeezed limit [cf. Eq. (73)]. This consistency relation is known to be valid in the standard slow roll inflationary scenarios (see App. D for a brief discussion on this point). But, we observe that, in all the ultra slow roll scenarios that we have considered, the aforementioned consistency relation is violated. This can be attributed to the fact that, in the ultra slow roll scenarios, in contrast to slow roll inflation, the amplitude of the curvature perturbation grows strongly on super-Hubble scales.

It would be interesting to investigate the manner in which the super-Hubble evolution of the long wavelength mode (the curvature perturbation in this case) modifies the consistency relation (for discussions on the scalar

bispectrum in such situations, see, for instance, Refs. [60, 61]). Rather than the pure ultra slow roll scenarios, it would be compelling to study the production of magnetic fields in inflationary models involving a brief phase of ultra slow roll sandwiched by two epochs of slow roll inflation. Such scenarios are in better agreement with the observations and would hence provide us with testable predictions. We defer these interesting possibilities to a future work.

ACKNOWLEDGMENTS

ST thanks the Indian Institute of Astrophysics, Bengaluru, India, for financial support through a postdoctoral fellowship. DC would like to thank the Indian Institute of Astrophysics, Bengaluru, India, and the Department of Science and Technology, Government of India, for support through the INSPIRE Faculty Fellowship grant DST/INSPIRE/04/2023/000110. DC would also like to thank the Indian Institute of Science, Bengaluru, India, for support through the C. V. Raman postdoctoral fellowship. HVR thanks the Raman Research Institute, Bengaluru, India, for support through a postdoctoral fellowship. HVR also acknowledges support by the MUR PRIN2022 Project ‘‘BROWSEPOL: Beyond standARd mOdel With coSMic microwavE background POLarization’’-2022EJNZ53 financed by the European Union—Next Generation EU. LS wishes to thank the Indo-French Centre for the Promotion of Advanced Research for support of the proposal 6704-4 under the Collaborative Scientific Research Programme.

Appendix A: Does the energy density of the electromagnetic field remain positive?

Earlier, in the case of the action in Eq. (34), which contains the non-conformal coupling of the form $J^2(X) \simeq J_0 X^{n/2}$, we had obtained the corresponding energy density ρ_{EM} of the electromagnetic field to be given by Eq. (39). While the expectation values $\langle \hat{\rho}_B \rangle$ and $\langle \hat{\rho}_E \rangle$ are clearly positive definite [cf. Eqs. (22), (23) and (24)], the quantity $\langle \hat{\rho}_{\text{EM}} \rangle$ contains n which may have either sign. This may raise the concern as to whether the total energy density of the electromagnetic field remains positive definite. To address the concern, let us study the behavior of the energy density of the electromagnetic field over the entire span of conformal time of our interest. For our choice of the non-conformal coupling function, i.e. $J = (\eta/\eta_e)^{n p/2}$ [cf. Eqs. (37) and (6)], we obtain the quantity \mathcal{A}_k describing the Fourier modes of the electromagnetic vector potential to be

$$\mathcal{A}_k(\eta) = \sqrt{-\frac{\pi \eta}{4}} e^{i[-(n p/2)+1]\pi/2} H_{-(n p-1)/2}^{(1)}(-k \eta), \quad (\text{A1})$$

where $H_\nu^{(1)}(z)$ denotes the Hankel functions of the first kind. On substituting this mode function in Eq. (24), we obtain the power spectra of the magnetic and electric fields to be

$$\mathcal{P}_B(k, \eta) = \frac{k^5}{2\pi^2 a^4} \left(-\frac{\pi\eta}{4}\right) \left|H_{-(n p-1)/2}^{(1)}(-k\eta)\right|^2, \quad (\text{A2})$$

$$\mathcal{P}_E(k, \eta) = \frac{k^5}{2\pi^2 a^4} \left(-\frac{\pi\eta}{4}\right) \left|H_{-(n p+1)/2}^{(1)}(-k\eta)\right|^2. \quad (\text{A3})$$

The expectation value of the total energy density of the electromagnetic field can be expressed as [cf. Eq. (39)]

$$\langle\hat{\rho}_{\text{EM}}(\eta)\rangle = \int_{k_{\text{min}}}^{k_{\text{max}}} d \ln k \langle\hat{\rho}_{\text{EM}}(k, \eta)\rangle, \quad (\text{A4})$$

where the expectation value of the energy density $\rho_{\text{EM}}(k, \eta)$ associated with a particular mode, say k , is given by

$$\langle\hat{\rho}_{\text{EM}}(k, \eta)\rangle = (1+2n)\mathcal{P}_E(k, \eta) + (1-2n)\mathcal{P}_B(k, \eta), \quad (\text{A5})$$

while k_{min} and k_{max} denote the smallest and largest wave numbers of observational interest. In our case, the expectation value of the energy density of the electromagnetic

field associated with a particular mode, say k , is given by

$$\begin{aligned} \langle\hat{\rho}_{\text{EM}}(k, \eta)\rangle = \frac{k^5 \eta}{8\pi^2 a^4} \left\{ \left|H_{-(n p+1)/2}^{(1)}(-k\eta)\right|^2 \right. \\ \left. + \left|H_{-(n p-1)/2}^{(1)}(-k\eta)\right|^2 \right. \\ \left. + 2n \left[\left|H_{-(n p+1)/2}^{(1)}(-k\eta)\right|^2 \right. \right. \\ \left. \left. - \left|H_{-(n p-1)/2}^{(1)}(-k\eta)\right|^2 \right] \right\}. \quad (\text{A6}) \end{aligned}$$

Let us now evaluate the above spectral energy density in the three ultra slow roll scenarios of interest. For the case when $p = 6$ and $n = -2/3$, we obtain that

$$\langle\hat{\rho}_{\text{EM}}(k, \eta)\rangle = \frac{H_1^4}{12\pi^2} (6k^4 \eta^4 + 20k^2 \eta^2 + 63). \quad (\text{A7})$$

For the second case, i.e. when $p = 4$ and $n = -1$, we obtain that

$$\langle\hat{\rho}_{\text{EM}}(k, \eta)\rangle = \frac{H_1^4}{4\pi^2} (2k^4 \eta^4 + 8k^2 \eta^2 + 27). \quad (\text{A8})$$

Finally, for the case wherein $p = 6$, $n = -1/3$ (discussed in App. D), we find that

$$\langle\hat{\rho}_{\text{EM}}(k, \eta)\rangle = \frac{H_1^4}{12\pi^2} k^2 \eta^2 (6k^2 \eta^2 + 5). \quad (\text{A9})$$

From the above three expressions, it is clear that the spectral energy density of the electromagnetic field $\langle\hat{\rho}_{\text{EM}}(k, \eta)\rangle$ is positive at all times for all the three cases. Therefore, the total electromagnetic energy density remains positive over the full span of time in all the three ultra slow roll scenarios of our interest.

Appendix B: The integrals

In Sec. V, we presented the results for the different contributions $\mathcal{B}_C(\mathbf{k}_1, \mathbf{k}_2, \mathbf{k}_3)$ to the three-point cross-correlation of interest in the scenario of pure ultra slow roll inflation for the cases of $p = 6$ and $p = 4$. We had considered the situation wherein $n p = -4$, which leads to a scale invariant spectrum for the magnetic field. To arrive at the different contributions, we needed to evaluate the integrals $\mathcal{G}_C(\mathbf{k}_1, \mathbf{k}_2, \mathbf{k}_3)$ [defined in Eqs. (54)] which depended on the background quantities such as the scale factor a , the Hubble parameter H , the first slow roll parameter ϵ_1 , and the mode functions f_k and \bar{A}_k that describe the curvature perturbations and the electromagnetic vector potential. Note that, we assume the scale factor to be of the de Sitter form with a constant Hubble parameter H_1 , while the first slow roll parameter ϵ_1 is given by Eq. (6). Moreover, the scalar mode functions f_k are given by Eqs. (12) and (14) (in the cases of $p = 6$ and $p = 4$, respectively), whereas the mode function associated with the electromagnetic vector potential \bar{A}_k is given by Eq. (40b). In this Appendix, we shall present the complete expressions for $\mathcal{G}_C(\mathbf{k}_1, \mathbf{k}_2, \mathbf{k}_3)$ arrived at using these functional forms.

1. Case of $p = 6$

When $p = 6$, we obtain the different integrals to be

$$\begin{aligned} \mathcal{G}_1(\mathbf{k}_1, \mathbf{k}_2, \mathbf{k}_3) = & -\frac{i H_1}{32 M_{\text{Pl}} \sqrt{k_1^3 k_2 k_3 \epsilon_{1i}} \eta_e} \left(\frac{\eta_i}{\eta_e}\right)^3 (k_1^2 - k_2^2 - k_3^2) \\ & \times \left(\left\{ 2i + 2(k_1 + k_2 + k_3) \eta_e + i [k_1^2 - 2k_1(k_2 + k_3) + (k_2 - k_3)^2] \eta_e^2 \right. \right. \\ & \left. \left. - (k_1 - k_2 - k_3)(k_1 + k_2 - k_3)(k_1 - k_2 + k_3) \eta_e^3 \right\} e^{i(k_1 + k_2 + k_3) \eta_e} \right. \\ & \left. + i(k_1 - k_2 - k_3)(k_1 + k_2 - k_3)(k_1 - k_2 + k_3)(k_1 + k_2 + k_3) \eta_e^4 \text{Ei}[i(k_1 + k_2 + k_3) \eta_e] \right), \end{aligned} \quad (\text{B1a})$$

$$\begin{aligned} \mathcal{G}_2(\mathbf{k}_1, \mathbf{k}_2, \mathbf{k}_3) = & -\frac{i H_1}{96 M_{\text{Pl}} k_1 \sqrt{k_1^3 k_2 k_3 \epsilon_{1i}} \eta_e} \left(\frac{\eta_i}{\eta_e}\right)^3 (k_1^2 - k_2^2 - k_3^2) \left(\left\{ 6i + 6(k_1 + k_2 + k_3) \eta_e \right. \right. \\ & \left. \left. - i [k_1^2 + 6k_1(k_2 + k_3) - 3(k_2 - k_3)^2] \eta_e^2 + [k_1^2 + 3(k_2 - k_3)^2] (k_1 - k_2 - k_3) \eta_e^3 \right\} e^{i(k_1 + k_2 + k_3) \eta_e} \right. \\ & \left. - i [k_1^4 + 2k_1^2(k_2^2 + k_3^2) - 3(k_2^2 - k_3^2)^2] \eta_e^4 \text{Ei}(i(k_1 + k_2 + k_3) \eta_e) \right), \end{aligned} \quad (\text{B1b})$$

$$\begin{aligned} \mathcal{G}_3(\mathbf{k}_1, \mathbf{k}_2, \mathbf{k}_3) = & -\frac{i H_1}{128 M_{\text{Pl}} \sqrt{k_1^3 k_2 k_3^5 \epsilon_{1i}} \eta_e} \left(\frac{\eta_i}{\eta_e}\right)^3 [2k_3^2(k_1^2 + k_2^2) + (k_1^2 - k_2^2)^2 - 3k_3^4] \\ & \times \left(\left\{ -6i - 6(k_1 + k_2 + k_3) \eta_e - i [-6k_3(k_1 + k_2) + 3(k_1 - k_2)^2 - k_3^2] \eta_e^2 \right. \right. \\ & \left. \left. + (k_1 + k_2 - k_3) [3(k_1 - k_2)^2 + k_3^2] \eta_e^3 \right\} e^{i(k_1 + k_2 + k_3) \eta_e} \right. \\ & \left. + i [2k_3^2(k_1^2 + k_2^2) - 3(k_1^2 - k_2^2)^2 + k_3^4] \eta_e^4 \text{Ei}[i(k_1 + k_2 + k_3) \eta_e] \right) + \mathbf{k}_2 \leftrightarrow \mathbf{k}_3, \end{aligned} \quad (\text{B1c})$$

$$\begin{aligned} \mathcal{G}_4(\mathbf{k}_1, \mathbf{k}_2, \mathbf{k}_3) = & -\frac{H_1 \sqrt{\epsilon_{1i}}}{16 M_{\text{Pl}} \sqrt{k_1^7 k_2 k_3^5} (k_1 + k_2 + k_3)^5 \eta_i^3} [(k_1^2 - k_2^2)^2 + 2(k_1^2 + k_2^2) k_3^2 - 3k_3^4] \\ & \times \left(\left\{ 3 \left[4k_1^5 + 23k_1^4(k_2 + k_3) + k_1^3(46k_2^2 + 107k_2k_3 + 51k_3^2) \right. \right. \right. \\ & \left. \left. \left. + k_1^2(42k_2^3 + 153k_2^2k_3 + 178k_2k_3^2 + 51k_3^3) \right. \right. \right. \\ & \left. \left. \left. + k_1(k_2 + k_3)(18k_2^3 + 69k_2^2k_3 + 84k_2k_3^2 + 23k_3^3) + (k_2 + k_3)^2(3k_2^3 + 12k_2^2k_3 + 15k_2k_3^2 + 4k_3^3) \right] \right. \right. \\ & \left. \left. - 3i(k_1 + k_2 + k_3) \left[k_1^5 + 8k_1^4(k_2 + k_3) + k_1^3(16k_2^2 + 47k_2k_3 + 21k_3^2) \right. \right. \right. \\ & \left. \left. \left. + k_1^2(k_2 + 3k_3)(12k_2^2 + 27k_2k_3 + 7k_3^2) + k_1(k_2 + k_3)(3k_2^3 + 24k_2^2k_3 + 39k_2k_3^2 + 8k_3^3) \right. \right. \right. \\ & \left. \left. \left. + k_3(k_2 + k_3)^2(3k_2^2 + 6k_2k_3 + k_3^2) \right] \eta_e - 3(k_1 + k_2 + k_3)^2 \left[k_1^4(k_2 + k_3) + 2k_1^3(k_2^2 + 5k_2k_3 + 2k_3^2) \right. \right. \right. \\ & \left. \left. \left. + k_1^2(k_2^3 + 12k_2^2k_3 + 23k_2k_3^2 + 4k_3^3) + k_1k_3(k_2 + k_3)(3k_2^2 + 9k_2k_3 + k_3^2) + k_2k_3^2(k_2 + k_3)^2 \right] \eta_e^2 \right. \right. \\ & \left. \left. + ik_1k_3(k_1 + k_2 + k_3)^3 \left[k_1^2(3k_2 + k_3) + k_1(3k_2^2 + 11k_2k_3 + k_3^2) + 3k_2k_3(k_2 + k_3) \right] \eta_e^3 \right. \right. \\ & \left. \left. + k_1^2k_2k_3^2(k_1 + k_2 + k_3)^4 \eta_e^4 \right\} e^{i(k_1 + k_2 + k_3) \eta_e} - 9(k_1 + k_2 + k_3)^5 \text{Ei}[i(k_1 + k_2 + k_3) \eta_e] \right) \\ & + \mathbf{k}_2 \leftrightarrow \mathbf{k}_3, \end{aligned} \quad (\text{B1d})$$

$$\mathcal{G}_5(\mathbf{k}_1, \mathbf{k}_2, \mathbf{k}_3) = -\frac{i H_1}{256 M_{\text{Pl}} \sqrt{k_1^3 k_2^5 k_3^5 \epsilon_{1i}} \eta_e^3} \left(\frac{\eta_i}{\eta_e}\right)^3 [k_1^4 - 2k_1^2(k_2^2 + k_3^2) + k_2^4 + 6k_2^2k_3^2 + k_3^4]$$

$$\begin{aligned}
& \times \left(\left\{ -24i - 24(k_1 + k_2 + k_3)\eta_e - 6i [k_1^2 - 4k_1(k_2 + k_3) - k_2^2 - 4k_2k_3 - k_3^2] \eta_e^2 \right. \right. \\
& + 2 [-3k_3(k_1^2 - 4k_1k_2 - k_2^2) + 3k_3^2(k_1 + k_2) + (k_1 - k_2)^3 - k_3^3] \eta_e^3 \\
& + i [2k_3^3(k_1 + k_2) - 2k_2k_3^2(3k_1 + k_2) - 2k_3(k_1 - k_2)^3 + (k_1 - k_2)^3(k_1 + k_2) - k_3^4] \eta_e^4 \\
& \left. - (k_1 - k_2 - k_3)(k_1 + k_2 - k_3)(k_1 - k_2 + k_3)(k_1^2 - k_2^2 - k_3^2) \eta_e^5 \right\} e^{i(k_1+k_2+k_3)\eta_e} \\
& + i(k_1 - k_2 - k_3)(k_1 + k_2 - k_3)(k_1 - k_2 + k_3)(k_1 + k_2 + k_3)(k_1^2 - k_2^2 - k_3^2) \eta_e^6 \\
& \times \text{Ei}[i(k_1 + k_2 + k_3)\eta_e] \Big), \tag{B1e}
\end{aligned}$$

$$\begin{aligned}
\mathcal{G}_6(\mathbf{k}_1, \mathbf{k}_2, \mathbf{k}_3) &= \frac{7iH_1}{768M_{\text{Pl}}\sqrt{k_1^3k_2^5k_3^5\epsilon_{1i}}\eta_e^3} \left(\frac{\eta_i}{\eta_e} \right)^3 [k_1^4 - 2k_1^2(k_2^2 + k_3^2) + k_2^4 + 6k_2^2k_3^2 + k_3^4] \\
& \times \left(3 \left\{ -24i - 24(k_1 + k_2 + k_3)\eta_e + 6i [k_1^2 + 4k_1(k_2 + k_3) + k_2^2 + 4k_2k_3 + k_3^2] \eta_e^2 \right. \right. \\
& - 2(k_1 + k_2 + k_3) [k_1^2 - 4k_1(k_2 + k_3) + k_2^2 - 4k_2k_3 + k_3^2] \eta_e^3 - i \left[k_1^4 - 2k_1^3(k_2 + k_3) \right. \\
& + 2k_1^2(k_2^2 + 3k_2k_3 + k_3^2) - 2k_1(k_2 + k_3)(k_2^2 - 4k_2k_3 + k_3^2) + (k_2 - k_3)^2(k_2^2 + k_3^2) \Big] \eta_e^4 \\
& \left. \left. + (k_1 - k_2 - k_3)(k_1 + k_2 - k_3)(k_1 - k_2 + k_3)(k_1^2 + k_2^2 + k_3^2) \eta_e^5 \right\} e^{i(k_1+k_2+k_3)\eta_e} \right. \\
& \left. - i [-3(k_1^2 + k_2^2)k_3^4 + 3(k_1^2 - k_2^2)^2(k_1^2 + k_2^2) - (3k_1^4 + 2k_1^2k_2^2 + 3k_2^4)k_3^2 + 3k_3^6] \eta_e^6 \right. \\
& \left. \times \text{Ei}[i(k_1 + k_2 + k_3)\eta_e] \right), \tag{B1f}
\end{aligned}$$

where $\text{Ei}(x)$ denotes the exponential integral function. We should mention that, in arriving at these results, we have regulated the oscillations that occur at the initial time in the sub-Hubble limit [i.e. when $(-k\eta_i) \gg 1$] by introducing an exponential cut-off, which is essential to single out the perturbative vacuum [96, 97, 99].

2. Case of $p = 4$

When $p = 4$, we obtain the different integrals to be

$$\begin{aligned}
\mathcal{G}_1(\mathbf{k}_1, \mathbf{k}_2, \mathbf{k}_3) &= -\frac{iH_1}{8M_{\text{Pl}}\sqrt{k_1k_2k_3\epsilon_{1i}}} \left(\frac{\eta_i}{\eta_e} \right)^2 (k_1^2 - k_2^2 - k_3^2) \left\{ [1 + i(k_1 - k_2 - k_3)\eta_e] e^{i(k_1+k_2+k_3)\eta_e} \right. \\
& \left. + (k_1^2 - k_2^2 - k_3^2) \eta_e^2 \text{Ei}[i(k_1 + k_2 + k_3)\eta_e] \right\}, \tag{B2a}
\end{aligned}$$

$$\begin{aligned}
\mathcal{G}_2(\mathbf{k}_1, \mathbf{k}_2, \mathbf{k}_3) &= -\frac{iH_1}{8M_{\text{Pl}}\sqrt{k_1k_2k_3\epsilon_{1i}}} \left(\frac{\eta_i}{\eta_e} \right)^2 (k_1^2 - k_2^2 - k_3^2) \left\{ \left[1 - i(k_1 + k_2 + k_3)\eta_e \right. \right. \\
& \left. \left. - \frac{2k_1k_2k_3\eta_e^2}{(k_1 + k_2 + k_3)} \right] e^{i(k_1+k_2+k_3)\eta_e} - (k_1^2 + k_2^2 + k_3^2) \eta_e^2 \text{Ei}[i(k_1 + k_2 + k_3)\eta_e] \right\}, \tag{B2b}
\end{aligned}$$

$$\begin{aligned}
\mathcal{G}_3(\mathbf{k}_1, \mathbf{k}_2, \mathbf{k}_3) &= \frac{iH_1}{32M_{\text{Pl}}\sqrt{k_1k_2k_3^5\epsilon_{1i}}} \left(\frac{\eta_i}{\eta_e} \right)^2 [2k_3^2(k_1^2 + k_2^2) + (k_1^2 - k_2^2)^2 - 3k_3^4] \\
& \times \left\{ \left[3 + 3i(k_1 - k_2 - k_3)\eta_e - \frac{2k_2k_3^2\eta_e^2}{(k_1 + k_2 + k_3)} \right] e^{i(k_1+k_2+k_3)\eta_e} \right. \\
& \left. + (3k_1^2 - 3k_2^2 - k_3^2) \eta_e^2 \text{Ei}[i(k_1 + k_2 + k_3)\eta_e] \right\} + \mathbf{k}_2 \leftrightarrow \mathbf{k}_3, \tag{B2c}
\end{aligned}$$

$$\mathcal{G}_4(\mathbf{k}_1, \mathbf{k}_2, \mathbf{k}_3) = -\frac{H_1\sqrt{\epsilon_{1i}}}{16M_{\text{Pl}}\sqrt{k_1^5k_2k_3^5}(k_1 + k_2 + k_3)^4\eta_i^2} [(k_1^2 - k_2^2)^2 + 2(k_1^2 + k_2^2)k_3^2 - 3k_3^4]$$

$$\begin{aligned}
& \times \left(\left\{ -i \left[3 k_3^2 (9 k_1^2 + 23 k_1 k_2 + 9 k_2^2) + 3 k_3 (k_1 + k_2) (5 k_1^2 + 14 k_1 k_2 + 5 k_2^2) \right. \right. \right. \\
& + 3 (k_1 + k_2)^2 (k_1^2 + 3 k_1 k_2 + k_2^2) + 19 k_3^3 (k_1 + k_2) + 4 k_3^4 \left. \left. \left. \right] \right. \right. \\
& - (k_1 + k_2 + k_3) \left[3 k_3^2 (3 k_1^2 + 11 k_1 k_2 + 3 k_2^2) + 3 k_3 (k_1 + k_2) (k_1^2 + 6 k_1 k_2 + k_2^2) \right. \\
& + 7 k_3^3 (k_1 + k_2) + 3 k_1 k_2 (k_1 + k_2)^2 + k_3^4 \left. \right] \eta_e + i k_3 (k_1 + k_2 + k_3)^2 \left[k_3 (k_1^2 + 8 k_1 k_2 + k_2^2) \right. \\
& + k_3^2 (k_1 + k_2) + 3 k_1 k_2 (k_1 + k_2) \left. \right] \eta_e^2 + k_1 k_2 k_3^2 (k_1 + k_2 + k_3)^3 \eta_e^3 \left. \right\} e^{i(k_1+k_2+k_3)\eta_e} \\
& + 3 i (k_1 + k_2 + k_3)^4 \text{Ei}[i(k_1 + k_2 + k_3)\eta_e] \left. \right) + \mathbf{k}_2 \leftrightarrow \mathbf{k}_3, \tag{B2d}
\end{aligned}$$

$$\begin{aligned}
\mathcal{G}_5(\mathbf{k}_1, \mathbf{k}_2, \mathbf{k}_3) &= -\frac{i H_1}{128 M_{\text{Pl}} \sqrt{k_1 k_2^5 k_3^5 \epsilon_{1i}} \eta_e^2} \left(\frac{\eta_i}{\eta_e} \right)^2 [k_1^4 - 2 k_1^2 (k_2^2 + k_3^2) + k_2^4 + 6 k_2^2 k_3^2 + k_3^4] \\
& \times \left(\left\{ -18 + 3 i [6 (k_2 + k_3) - 2 k_1] \eta_e + 3 [k_1^2 - 2 k_1 (k_2 + k_3) + k_2^2 + 6 k_2 k_3 + k_3^2] \eta_e^2 \right. \right. \\
& + 3 i (k_1 - k_2 - k_3) (k_1 + k_2 - k_3) (k_1 - k_2 + k_3) \eta_e^3 \left. \left. \right\} e^{i(k_1+k_2+k_3)\eta_e} \right. \\
& + [2 k_3^2 (k_2^2 - 3 k_1^2) + 3 (k_1^2 - k_2^2)^2 + 3 k_3^4] \eta_e^4 \text{Ei}[i(k_1 + k_2 + k_3)\eta_e] \left. \right), \tag{B2e}
\end{aligned}$$

$$\begin{aligned}
\mathcal{G}_6(\mathbf{k}_1, \mathbf{k}_2, \mathbf{k}_3) &= \frac{3 i H_1}{128 M_{\text{Pl}} \sqrt{k_1 k_2^5 k_3^5 \epsilon_{1i}} \eta_e^2} \left(\frac{\eta_i}{\eta_e} \right)^2 [k_1^4 - 2 k_1^2 (k_2^2 + k_3^2) + k_2^4 + 6 k_2^2 k_3^2 + k_3^4] \\
& \times \left(\left\{ -18 + 18 i (k_1 + k_2 + k_3) \eta_e - 3 [3 k_1^2 - 6 k_1 (k_2 + k_3) - k_2^2 - 6 k_2 k_3 - k_3^2] \eta_e^2 \right. \right. \\
& - \frac{3 i}{(k_1 + k_2 + k_3)} [3 k_1^4 - 2 k_1^2 (k_2^2 + k_3^2) + 8 k_1 k_2 k_3 (k_2 + k_3) - (k_2^2 - k_3^2)^2] \eta_e^3 \\
& - \left. \left. \frac{8 k_1 k_2^2 k_3^2 \eta_e^4}{(k_1 + k_2 + k_3)} \right\} e^{i(k_1+k_2+k_3)\eta_e} \right. \\
& - [9 k_1^4 - 6 k_1^2 (k_2^2 + k_3^2) - 3 k_2^4 - 2 k_2^2 k_3^2 - 3 k_3^4] \eta_e^4 \text{Ei}[i(k_1 + k_2 + k_3)\eta_e] \left. \right). \tag{B2f}
\end{aligned}$$

We should mention that the expressions listed above have been arrived at without any approximations. In Sec. V, we have used these $\mathcal{G}_C(\mathbf{k}_1, \mathbf{k}_2, \mathbf{k}_3)$ to evaluate the contributions $\mathcal{B}_C(\mathbf{k}_1, \mathbf{k}_2, \mathbf{k}_3)$. We should add that, in listing the different contributions $\mathcal{B}_C(\mathbf{k}_1, \mathbf{k}_2, \mathbf{k}_3)$, we have retained only the leading order terms in η_e .

Appendix C: Non-Gaussian contributions to $\mathcal{P}_B(k)$

Since $b_{\text{NL}}(\mathbf{k}_1, \mathbf{k}_2, \mathbf{k}_3)$ attains large values for $p = 4$, we may expect a strong non-Gaussian contribution to the power spectrum $\mathcal{P}_B(k)$ of the magnetic field. This contribution can potentially alter the shape of the spectrum. In this appendix, we shall inspect such a possibility for the cases of $p = 6$ and $p = 4$ and values of n that lead to a scale invariant power spectrum for the magnetic field. Specifically, we shall arrive at an approximate estimate of the non-Gaussian contributions.

We should mention here that similar analyses in the case of the contributions to the scalar power spectrum $\mathcal{P}_S(k)$ due to the scalar non-Gaussianity parameter $f_{\text{NL}}(\mathbf{k}_1, \mathbf{k}_2, \mathbf{k}_3)$ has been carried out earlier [50, 51, 117–

119]. We shall suitably adopt the method followed in the case of the scalar power spectrum (in this context, see Refs. [51, 119]). Using the defining relation in Eq. (55), we can express the power spectrum of the magnetic field that is modified due to the non-Gaussianity parameter $b_{\text{NL}}(\mathbf{k}_1, \mathbf{k}_2, \mathbf{k}_3)$ to be

$$\begin{aligned}
\mathcal{P}_B^{\text{M}}(k) &= \mathcal{P}_B(k) + \frac{k^3}{4\pi} \int d^3 \mathbf{q} b_{\text{NL}}^2(q, |\mathbf{k} - \mathbf{q}|, k) \\
& \times \frac{\mathcal{P}_S(q) \mathcal{P}_B(|\mathbf{k} - \mathbf{q}|)}{q^3 |\mathbf{k} - \mathbf{q}|^3} \\
& = \mathcal{P}_B^0 \left[1 + \frac{k^3}{4\pi} \int d^3 \mathbf{q} b_{\text{NL}}^2(q, |\mathbf{k} - \mathbf{q}|, k) \right. \\
& \left. \times \frac{\mathcal{P}_S(q)}{q^3 |\mathbf{k} - \mathbf{q}|^3} \right]. \tag{C1}
\end{aligned}$$

In arriving at the second equation we have used the fact that $\mathcal{P}_B(k) = \mathcal{P}_B^0$, i.e. we have a scale-invariant amplitude for the power spectrum of the magnetic field in both the cases of $p = 6$ and 4 . The second term in the expression within the square braces is the non-Gaussian contribution to the power spectrum of the magnetic field, which arises due to the interaction with the scalar perturbations. Note that the contribution is proportional to the product of the square of the non-Gaussianity parameter $b_{\text{NL}}(\mathbf{k}_1, \mathbf{k}_2, \mathbf{k}_3)$ and the scalar power spectrum $\mathcal{P}_s(k)$.

Recall that, in the case of $p = 6$, we found that the quantity $b_{\text{NL}}(\mathbf{k}_1, \mathbf{k}_2, \mathbf{k}_3)$ peaks in the flattened limit [cf. Fig. 1]. This behavior is similar to the orthogonal template of the scalar bispectrum that is often used to characterize the scalar non-Gaussianity parameter $f_{\text{NL}}(\mathbf{k}_1, \mathbf{k}_2, \mathbf{k}_3)$ (see, for instance, Refs. [119–122]). Hence, as a reliable approximation, we can use the orthogonal template for $b_{\text{NL}}(\mathbf{k}_1, \mathbf{k}_2, \mathbf{k}_3)$ to calculate the integral that describes the non-Gaussian contribution to $\mathcal{P}_B^M(k)$. In other words, we shall set $b_{\text{NL}}(\mathbf{k}_1, \mathbf{k}_2, \mathbf{k}_3) = b_{\text{NL}}^{\text{ortho}} \mathcal{F}^{\text{ortho}}(k_1, k_2, k_3)$, where $b_{\text{NL}}^{\text{ortho}}$ and the function $\mathcal{F}^{\text{ortho}}(k_1, k_2, k_3)$ describes the orthogonal shape [120, 121]. We shall set the overall amplitude to be $b_{\text{NL}}^{\text{ortho}} = 16$, which is the maximum value that the non-Gaussianity parameter attains in the flattened limit. We also use the scale invariant behavior of the scalar power spectrum in this case, i.e. we set $\mathcal{P}_s(k) = \mathcal{P}_s(k_*)$. Under these conditions, the integral simplifies to

$$\mathcal{P}_B^M(k) = \mathcal{P}_B^0 \left[1 + \mathcal{P}_s(k_*) \frac{(b_{\text{NL}}^{\text{ortho}})^2}{4\pi} \mathcal{I}^{\text{ortho}} \right], \quad (\text{C2})$$

where $\mathcal{I}^{\text{ortho}}$ is the value of the integral performed with the orthogonal template of the non-Gaussianity parameter and its typical value is $\mathcal{I}^{\text{ortho}} \sim 10^{-2}$ (for the relevant calculational details of the integral, see Ref. [119]). Using the values of $\mathcal{P}_s(k_*)$, $b_{\text{NL}}^{\text{ortho}}$ and $\mathcal{I}^{\text{ortho}}$, we obtain the modification to the power spectrum of the magnetic field power due to the second term above to be

$$\frac{\mathcal{P}_B^M(k) - \mathcal{P}_B^0}{\mathcal{P}_B^0} \simeq 4 \times 10^{-10}. \quad (\text{C3})$$

This implies that the non-Gaussian contribution to the magnetic power spectrum is very small in the case of $p = 6$.

On the other hand, in the case of $p = 4$, the quantity $b_{\text{NL}}(\mathbf{k}_1, \mathbf{k}_2, \mathbf{k}_3)$ has a similar orthogonal shape, except that there is an overall amplification of $1/\eta_e^2$. This behavior of the non-Gaussianity parameter makes the $p = 4$ scenario more interesting than the $p = 6$ scenario. While $\mathcal{P}_B(k) = \mathcal{P}_B^0$ in this case as well, the scalar power spectrum has a strong scale dependence and behaves as

$$\mathcal{P}_s(k) = \mathcal{P}_s(k_*) \left(\frac{k}{k_*} \right)^2, \quad (\text{C4})$$

where $\mathcal{P}_s(k_*)$ is normalized to the CMB value at the pivot scale, as we discussed earlier while arriving at a

suitable value of H_1 . Although $b_{\text{NL}}(\mathbf{k}_1, \mathbf{k}_2, \mathbf{k}_3)$ can be approximated well by the orthogonal template as in the previous case, the scale dependence of $\mathcal{P}_s(k)$ makes the integral non-trivial to calculate. So, we shall explicitly evaluate the contribution below.

The modification to the power spectrum of the magnetic field or, in other words, the relative difference between $\mathcal{P}_B^M(k)$ and \mathcal{P}_B^0 can be expressed in terms of $\mathcal{P}_s(k_*)$ and $b_{\text{NL}}(\mathbf{k}_1, \mathbf{k}_2, \mathbf{k}_3)$ as follows:

$$\begin{aligned} \frac{\mathcal{P}_B^M(k) - \mathcal{P}_B^0}{\mathcal{P}_B^0} &= \frac{k^3}{4\pi} \mathcal{P}_s(k_*) \int d^3\mathbf{q} \left(\frac{q}{k_*} \right)^2 \\ &\quad \times \frac{b_{\text{NL}}^2(q, |\mathbf{k} - \mathbf{q}|, k)}{q^3 |\mathbf{k} - \mathbf{q}|^3}, \\ &= \frac{k^3}{2k_*^2} \mathcal{P}_s(k_*) \int d \ln q q^2 \\ &\quad \int d \cos \theta \frac{b_{\text{NL}}^2(q, |\mathbf{k} - \mathbf{q}|, k)}{|\mathbf{k} - \mathbf{q}|^3}, \end{aligned} \quad (\text{C5})$$

where we have simplified the angular integral by aligning \mathbf{k} along the z -direction in \mathbf{q} space. Further, we can introduce the dimensionless variables $x = q/k$ and $y = |\mathbf{k} - \mathbf{q}|/k$, so that the above expression reduces to

$$\begin{aligned} \frac{\mathcal{P}_B^M(k) - \mathcal{P}_B^0}{\mathcal{P}_B^0} &= \frac{\mathcal{P}_s(k_*)}{2} \left(\frac{k}{k_*} \right)^2 \\ &\quad \times \int_0^\infty dx \int_{|1-x|}^{1+x} dy \frac{b_{\text{NL}}^2(kx, ky, k)}{y^2}. \end{aligned} \quad (\text{C6})$$

We utilize the behavior of $b_{\text{NL}}(\mathbf{k}_1, \mathbf{k}_2, \mathbf{k}_3)$ peaking in the flattened limit to restrict the limits of the integrals in the x - y plane. This is done to simplify the integration and yet obtain a reasonably good estimate of $\mathcal{P}_B^M(k)$. Note that, while the wave number corresponding to the scalar perturbation is q , the wave numbers of the modes of the magnetic field are k and $|\mathbf{k} - \mathbf{q}|$. Therefore, the range of x is determined by the range of q in the flattened limit. The flattened limit corresponds to the right edge of the triangular region in Fig. 1, along the line $k_2/k_3 = k_1/k_3 + 1$. From the figure, we can see that the wave number of scalar perturbation k_1 (which is q in the integral) ranges from k_3 to $2k_3$ along this limit, where k_3 (akin to k in the integral above) is the wave number corresponding to the modes of the magnetic field. This sets the range of x to be $[1, 2]$. Similarly, the range of k_2 (equivalent to $|\mathbf{k} - \mathbf{q}|$) in this regime is from 0 to k_3 and hence the range of y corresponds to $[0, 1+x]$. Hence, the integrals are restricted to

$$\begin{aligned} \frac{\mathcal{P}_B^M(k) - \mathcal{P}_B^0}{\mathcal{P}_B^0} &= \frac{\mathcal{P}_s(k_*)}{2} \left(\frac{k}{k_*} \right)^2 \\ &\quad \times \int_1^2 dx \int_0^{1+x} dy \frac{b_{\text{NL}}^2(kx, ky, k)}{y^2}. \end{aligned} \quad (\text{C7})$$

Further, we use the property that $b_{\text{NL}}(\mathbf{k}_1, \mathbf{k}_2, \mathbf{k}_3) \propto 1/(k_3 \eta_e)^2$ in this limit. This greatly simplifies the in-

tegral, which can then be evaluated to be

$$\begin{aligned} \frac{\mathcal{P}_B^M(k) - \mathcal{P}_B^0}{\mathcal{P}_B^0} &= \frac{\mathcal{P}_S(k_*)}{2} \left(\frac{k}{k_*}\right)^2 \\ &\times \left(\frac{b_{\text{NL}}^{\text{ortho}}}{k^2 \eta_e^2}\right)^2 \int_1^2 dx \int_0^{1+x} \frac{dy}{y^2} \\ &\simeq \frac{\mathcal{P}_S(k_*)}{2} \left(\frac{k}{k_*}\right)^2 \left(\frac{b_{\text{NL}}^{\text{ortho}}}{k^2 \eta_e^2}\right)^2 \\ &\times \left(\frac{1}{y_{\text{min}}} - \ln 2\right), \end{aligned} \quad (\text{C8})$$

where we have set the lower limit of the y -integral to be a small finite value $k_{\text{min}}/k = y_{\text{min}} = 10^{-2}$ instead of zero, to regulate the divergence that arises. Note that, in the above expression, we can set $b_{\text{NL}}^{\text{ortho}} \simeq 10$, which is roughly the amplitude of the parameter in the flattened limit apart from the $1/(k^2 \eta_e^2)$ factor, as can be seen from Fig. 1.

It should be clear from the above expression that the relative difference is much larger than unity, mainly because of the presence of the factor $1/(k \eta_e)^4$. Therefore, the non-Gaussian contribution to $\mathcal{P}_B(k)$ dominates over \mathcal{P}_B^0 in the case of $p = 4$. Such a modified $\mathcal{P}_B^M(k)$ can be expressed as

$$\begin{aligned} \mathcal{P}_B^M(k) &\simeq \frac{\mathcal{P}_B^0 \mathcal{P}_S(k_*)}{2 y_{\text{min}}} \frac{(b_{\text{NL}}^{\text{ortho}})^2}{k^2 k_*^2 \eta_e^4} \\ &\simeq 1.5 \times 10^{-63} \left(\frac{k_*}{k}\right)^2 M_{\text{Pl}}^4. \end{aligned} \quad (\text{C9})$$

Note that $\mathcal{P}_B^0 \simeq 9 H_1^4 / (4 \pi^2) \simeq 8.9 \times 10^{-140} M_{\text{Pl}}^4$. So, it is clear that $\mathcal{P}_B^M(k)$ is dominated by the non-Gaussian contribution. Moreover, $b_{\text{NL}}(\mathbf{k}_1, \mathbf{k}_2, \mathbf{k}_3)$ introduces a strong scale dependence as $\mathcal{P}_B^M(k) \propto 1/k^2$, unlike the strictly scale invariant \mathcal{P}_B^0 . While, the overall amplitude is still much smaller than required around k_* , it can lead to large contributions over larger scales such that $k \ll k_*$.

Appendix D: Non-Gaussianity parameter in other cases

To further investigate the validity of the consistency relation given in Eq. (73), let us consider the ultra slow roll scenario wherein $p = 6$ with $n = -1/3$. In this case, since $np = -2$, the power spectrum of the magnetic field is not scale invariant but instead has a strong blue tilt and behaves as k^2 (i.e. $n_B = 2$). Moreover, in this case, we find that the contributions to the cross-correlation from the terms $\mathcal{B}_1(\mathbf{k}_1, \mathbf{k}_2, \mathbf{k}_3)$, $\mathcal{B}_2(\mathbf{k}_1, \mathbf{k}_2, \mathbf{k}_3)$, $\mathcal{B}_3(\mathbf{k}_1, \mathbf{k}_2, \mathbf{k}_3)$, $\mathcal{B}_5(\mathbf{k}_1, \mathbf{k}_2, \mathbf{k}_3)$, and $\mathcal{B}_6(\mathbf{k}_1, \mathbf{k}_2, \mathbf{k}_3)$ are of the same order. At the leading order, the resulting non-

Gaussianity parameter can be obtained to be

$$\begin{aligned} b_{\text{NL}}(\mathbf{k}_1, \mathbf{k}_2, \mathbf{k}_3) &= \frac{\eta_e^2}{12 k_2^2 k_3^2 (k_2 + k_3)} \left[k_1^7 \right. \\ &\quad + 6 k_1^2 k_2^2 k_3^2 (k_2 + k_3) - 2 k_1^5 (k_2^2 + k_3^2) \\ &\quad - 6 k_2^2 k_3^2 (k_2 + k_3) (k_2^2 + k_3^2) \\ &\quad \left. + k_1^3 (k_2^4 + 6 k_2^2 k_3^2 + k_3^4) \right]. \end{aligned} \quad (\text{D1})$$

In Fig. 2, we have plotted the above non-Gaussianity parameter as a density plot for an arbitrary configuration of wave vectors, in the same manner as we have done earlier. Since the absolute values of the numbers involved are very small, we have divided the quantity $b_{\text{NL}}(\mathbf{k}_1, \mathbf{k}_2, \mathbf{k}_3)$ by $(k_*^2 \eta_e^2)$, where $k_* = 0.05 \text{ Mpc}^{-1}$, i.e. the pivot scale. When $(-k_* \eta_e) \ll 1$, in the equilateral, flattened and squeezed limits, we find that the non-Gaussianity parameter reduces to

$$\frac{b_{\text{NL}}^{\text{eq}}(k_*)}{k_*^2 \eta_e^2} = -\frac{7}{24} = -0.29, \quad (\text{D2a})$$

$$\frac{b_{\text{NL}}^{\text{fl}}(k_*)}{k_*^2 \eta_e^2} = \frac{11}{3} = 3.67, \quad (\text{D2b})$$

$$\frac{b_{\text{NL}}^{\text{sq}}(k_*)}{k_*^2 \eta_e^2} \simeq -1. \quad (\text{D2c})$$

These numbers can be matched with the plot in Fig. 2. In this case, it is important to note that, contrary to the previous two cases, the values of $b_{\text{NL}}(\mathbf{k}_1, \mathbf{k}_2, \mathbf{k}_3)$ are very small. Interestingly, the value is smaller in the equilateral limit than in the squeezed limit. Moreover, the non-Gaussianity parameter does not vanish in the squeezed limit (though it proves to be rather small).

Let us now compare the $b_{\text{NL}}(\mathbf{k}_1, \mathbf{k}_2, \mathbf{k}_3)$ we have obtained in the ultra slow roll scenarios of interest with the results arrived at in the standard slow roll inflationary scenario. In the latter case, as is often done, we shall assume that the electromagnetic field is described by the action in Eq. (16) with a non-conformal coupling function of the form $J(\phi)$. For the slow roll case, in a background that is approximated to be that of de Sitter, and with a non-conformal coupling function that behaves as $J \propto a^2$ [i.e. when $\bar{n} = 2$, cf. Eqs. (25) and (26)], we obtain a scale invariant power spectrum for the magnetic field (i.e. $n_B = 0$). Also, in this case, the three-point cross-correlation of interest and the corresponding non-Gaussianity parameter can be easily calculated (for details, see Refs. [92, 103]). For suitable choices of parameters such that the inflationary scalar power spectrum is normalized to the value suggested by the CMB (say, when $\epsilon_1 \simeq 10^{-3}$ and $\eta_e = -10^{-19} \text{ Mpc}$), we obtain the following estimates for $b_{\text{NL}}(\mathbf{k}_1, \mathbf{k}_2, \mathbf{k}_3)$ in the various limits of wave numbers (when evaluated at the pivot scale):

$$b_{\text{NL}}^{\text{eq}}(k_*) \simeq 180.18, \quad (\text{D3a})$$

$$b_{\text{NL}}^{\text{fl}}(k_*) \simeq 2249.50, \quad (\text{D3b})$$

$$b_{\text{NL}}^{\text{sq}}(k_*) = 2. \quad (\text{D3c})$$

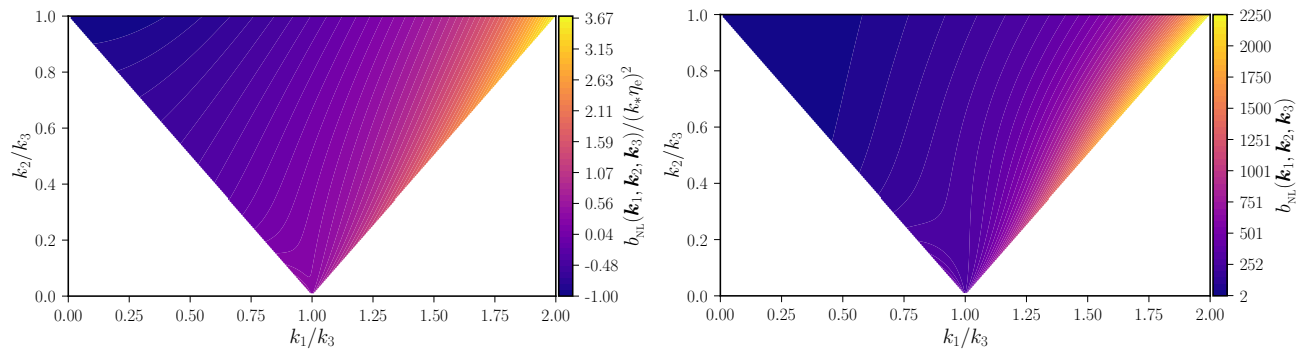


FIG. 2. Density plots of the non-Gaussianity parameter $b_{\text{NL}}(\mathbf{k}_1, \mathbf{k}_2, \mathbf{k}_3)$ in the ultra slow roll scenario with $p = 6$ and $n = -1/3$ (on the left) and slow roll inflation (on the right). In the ultra slow roll case, we have chosen the parameter values to be $\epsilon_{1i} = 10^{-3}$, $\eta_i = -10^6$ Mpc and $\eta_e = -10^{-19}$ Mpc, as in the previous figure. To arrive at the results in the slow roll case, we have assumed the non-conformal coupling function to be of the form $J(\phi)$, as in the action in Eq. (16). Moreover, we have assumed that $J \propto a^2$, corresponding to $\bar{n} = 2$, which leads to a scale invariant power spectrum for the magnetic field. Also, we have chosen the values of the parameters to be $\epsilon_{1i} = 10^{-3}$, $H_1 = 1.25 \times 10^{-5} M_{\text{Pl}}$ and $\eta_e = -10^{-19}$ Mpc. Lastly, we have set k_3 to be the pivot scale k_* in both the cases.

Note that in order to arrive at these numbers, we have neglected the contribution due to the term $\mathcal{B}_4(\mathbf{k}_1, \mathbf{k}_2, \mathbf{k}_3)$, since this term, being directly proportional to the first slow roll parameter ϵ_1 , would be subdominant compared to the other terms. These numbers can be matched with the density plot in Fig. 2, where we have plotted $b_{\text{NL}}(\mathbf{k}_1, \mathbf{k}_2, \mathbf{k}_3)$ for an arbitrary triangular configuration of wave vectors. It is also clear from the above-mentioned value of $b_{\text{NL}}^{\text{sq}}(k)$ that the consistency relation in Eq. (73) is satisfied in this case (since $n_{\text{B}} = 0$).

Finally, if we consider another slow roll case in an approximately de Sitter background with $J(\phi) \propto a$ (corresponding to $\bar{n} = 1$), we obtain that $\mathcal{P}_{\text{B}}(k) \propto k^2$ [i.e.

$n_{\text{B}} = 2$, cf. Eq. (32)]. Evaluating the three-point function in this scenario leads to the following values of the non-Gaussianity parameter $b_{\text{NL}}(\mathbf{k}_1, \mathbf{k}_2, \mathbf{k}_3)$ in the different limits of wave numbers (when $\epsilon_1 \simeq 10^{-3}$ and $\eta_e = -10^{-19}$ Mpc):

$$b_{\text{NL}}^{\text{eq}}(k) \simeq 0.96, \quad (\text{D4a})$$

$$b_{\text{NL}}^{\text{fl}}(k) \simeq 3, \quad (\text{D4b})$$

$$b_{\text{NL}}^{\text{sq}}(k) = 1. \quad (\text{D4c})$$

As in the preceding case, it is evident from the above value of $b_{\text{NL}}^{\text{sq}}(k)$ that the consistency relation in Eq. (73) is satisfied in this case as well.

-
- [1] D. Grasso and H. R. Rubinstein, Phys. Rept. **348**, 163 (2001), arXiv:astro-ph/0009061.
- [2] M. Giovannini, Int. J. Mod. Phys. D **13**, 391 (2004), arXiv:astro-ph/0312614.
- [3] A. Brandenburg and K. Subramanian, Phys. Rept. **417**, 1 (2005), arXiv:astro-ph/0405052.
- [4] R. M. Kulsrud and E. G. Zweibel, **71**, 0046091 (2008), arXiv:0707.2783 [astro-ph].
- [5] K. Subramanian, Astron. Nachr. **331**, 110 (2010), arXiv:0911.4771 [astro-ph.CO].
- [6] A. Kandus, K. E. Kunze, and C. G. Tsagas, Phys. Rept. **505**, 1 (2011), arXiv:1007.3891 [astro-ph.CO].
- [7] L. M. Widrow, D. Ryu, D. R. G. Schleicher, K. Subramanian, C. G. Tsagas, and R. A. Treumann, Space Sci. Rev. **166**, 37 (2012), arXiv:1109.4052 [astro-ph.CO].
- [8] R. Durrer and A. Neronov, Astron. Astrophys. Rev. **21**, 62 (2013), arXiv:1303.7121 [astro-ph.CO].
- [9] K. Subramanian, Rept. Prog. Phys. **79**, 076901 (2016), arXiv:1504.02311 [astro-ph.CO].
- [10] T. Vachaspati 10.1088/1361-6633/ac03a9 (2020), arXiv:2010.10525 [astro-ph.CO].
- [11] A. Neronov and I. Vovk, Science **328**, 73 (2010), arXiv:1006.3504 [astro-ph.HE].
- [12] F. Tavecchio, G. Ghisellini, L. Foschini, G. Bonnoli, G. Ghirlanda, and P. Coppi, Mon. Not. Roy. Astron. Soc. **406**, L70 (2010), arXiv:1004.1329 [astro-ph.CO].
- [13] K. Dolag, M. Kachelriess, S. Ostapchenko, and R. Tomas, Astrophys. J. Lett. **727**, L4 (2011), arXiv:1009.1782 [astro-ph.HE].
- [14] C. D. Dermer, M. Cavadini, S. Razzaque, J. D. Finck, J. Chiang, and B. Lott, Astrophys. J. Lett. **733**, L21 (2011), arXiv:1011.6660 [astro-ph.HE].
- [15] I. Vovk, A. M. Taylor, D. Semikoz, and A. Neronov, Astrophys. J. Lett. **747**, L14 (2012), arXiv:1112.2534 [astro-ph.CO].
- [16] A. Taylor, I. Vovk, and A. Neronov, Astron. Astrophys. **529**, A144 (2011), arXiv:1101.0932 [astro-ph.HE].
- [17] K. Takahashi, M. Mori, K. Ichiki, and S. Inoue, Astrophys. J. Lett. **744**, L7 (2012), arXiv:1103.3835 [astro-ph.CO].
- [18] T. Papanikolaou and K. N. Gourgouliatos, Phys. Rev. D **107**, 103532 (2023), arXiv:2301.10045 [astro-ph.CO].
- [19] T. Papanikolaou and K. N. Gourgouliatos, Phys. Rev. D **108**, 063532 (2023), arXiv:2306.05473 [astro-ph.CO].

- [20] R. Durrer, P. G. Ferreira, and T. Kahniashvili, *Phys. Rev. D* **61**, 043001 (2000), arXiv:astro-ph/9911040.
- [21] M. Giovannini and K. E. Kunze, *Phys. Rev. D* **77**, 063003 (2008), arXiv:0712.3483 [astro-ph].
- [22] F. Finelli, F. Paci, and D. Paoletti, *Phys. Rev. D* **78**, 023510 (2008), arXiv:0803.1246 [astro-ph].
- [23] D. Paoletti, F. Finelli, and F. Paci, *Mon. Not. Roy. Astron. Soc.* **396**, 523 (2009), arXiv:0811.0230 [astro-ph].
- [24] J. R. Shaw and A. Lewis, *Phys. Rev. D* **81**, 043517 (2010), arXiv:0911.2714 [astro-ph.CO].
- [25] C. Bonvin, C. Caprini, and R. Durrer, *Phys. Rev. D* **88**, 083515 (2013), arXiv:1308.3348 [astro-ph.CO].
- [26] M. Ballardini, F. Finelli, and D. Paoletti, *JCAP* **10**, 031, arXiv:1412.1836 [astro-ph.CO].
- [27] J. R. Shaw and A. Lewis, *Phys. Rev. D* **86**, 043510 (2012), arXiv:1006.4242 [astro-ph.CO].
- [28] D. Paoletti and F. Finelli, *Phys. Rev. D* **83**, 123533 (2011), arXiv:1005.0148 [astro-ph.CO].
- [29] P. A. R. Ade *et al.* (Planck), *Astron. Astrophys.* **594**, A19 (2016), arXiv:1502.01594 [astro-ph.CO].
- [30] A. Zucca, Y. Li, and L. Pogosian, *Phys. Rev. D* **95**, 063506 (2017), arXiv:1611.00757 [astro-ph.CO].
- [31] D. Paoletti, J. Chluba, F. Finelli, and J. A. Rubino-Martin, *Mon. Not. Roy. Astron. Soc.* **484**, 185 (2019), arXiv:1806.06830 [astro-ph.CO].
- [32] D. Paoletti and F. Finelli, *JCAP* **11**, 028, arXiv:1910.07456 [astro-ph.CO].
- [33] D. Paoletti, J. Chluba, F. Finelli, and J. A. Rubiño Martin, *MNRAS* **10.1093/mnras/stac2947** (2022), arXiv:2204.06302 [astro-ph.CO].
- [34] M. S. Turner and L. M. Widrow, *Phys. Rev. D* **37**, 2743 (1988).
- [35] B. Ratra, *Astrophys. J. Lett.* **391**, L1 (1992).
- [36] K. Bamba and J. Yokoyama, *Phys. Rev. D* **69**, 043507 (2004), arXiv:astro-ph/0310824.
- [37] J. Martin and J. Yokoyama, *JCAP* **01**, 025, arXiv:0711.4307 [astro-ph].
- [38] M.-a. Watanabe, S. Kanno, and J. Soda, *Phys. Rev. Lett.* **102**, 191302 (2009), arXiv:0902.2833 [hep-th].
- [39] S. Kanno, J. Soda, and M.-a. Watanabe, *JCAP* **12**, 009, arXiv:0908.3509 [astro-ph.CO].
- [40] T. Markkanen, S. Nurmi, S. Rasanen, and V. Vennin, *JCAP* **06**, 035, arXiv:1704.01343 [astro-ph.CO].
- [41] R. Abbott *et al.* (LIGO Scientific, Virgo), *Astrophys. J. Lett.* **913**, L7 (2021), arXiv:2010.14533 [astro-ph.HE].
- [42] V. De Luca, G. Franciolini, P. Pani, and A. Riotto, *JCAP* **06**, 044, arXiv:2005.05641 [astro-ph.CO].
- [43] K. Jedamzik, *JCAP* **09**, 022, arXiv:2006.11172 [astro-ph.CO].
- [44] K. Jedamzik, *Phys. Rev. Lett.* **126**, 051302 (2021), arXiv:2007.03565 [astro-ph.CO].
- [45] G. Franciolini, V. Baibhav, V. De Luca, K. K. Y. Ng, K. W. K. Wong, E. Berti, P. Pani, A. Riotto, and S. Vitale, (2021), arXiv:2105.03349 [gr-qc].
- [46] D. K. Hazra, L. Sriramkumar, and J. Martin, *JCAP* **05**, 026, arXiv:1201.0926 [astro-ph.CO].
- [47] V. Sreenath, D. K. Hazra, and L. Sriramkumar, *JCAP* **02**, 029, arXiv:1410.0252 [astro-ph.CO].
- [48] V. Atal and C. Germani, *Phys. Dark Univ.* **24**, 100275 (2019), arXiv:1811.07857 [astro-ph.CO].
- [49] V. Atal, J. Cid, A. Escrivà, and J. Garriga, *JCAP* **05**, 022, arXiv:1908.11357 [astro-ph.CO].
- [50] H. V. Ragavendra, P. Saha, L. Sriramkumar, and J. Silk, *Phys. Rev. D* **103**, 083510 (2021), arXiv:2008.12202 [astro-ph.CO].
- [51] H. V. Ragavendra, *Phys. Rev. D* **105**, 063533 (2022), arXiv:2108.04193 [astro-ph.CO].
- [52] Y.-F. Cai, X.-H. Ma, M. Sasaki, D.-G. Wang, and Z. Zhou, *JCAP* **12**, 034, arXiv:2207.11910 [astro-ph.CO].
- [53] H. V. Ragavendra and L. Sriramkumar, *Galaxies* **11**, 34 (2023), arXiv:2301.08887 [astro-ph.CO].
- [54] M. H. Namjoo and B. Nikbakht, *JCAP* **08**, 005, arXiv:2401.12958 [astro-ph.CO].
- [55] S. Tripathy, D. Chowdhury, R. K. Jain, and L. Sriramkumar, *Phys. Rev. D* **105**, 063519 (2022), arXiv:2111.01478 [astro-ph.CO].
- [56] S. Tripathy, D. Chowdhury, H. V. Ragavendra, R. K. Jain, and L. Sriramkumar, *Phys. Rev. D* **107**, 043501 (2023), arXiv:2211.05834 [astro-ph.CO].
- [57] M. H. Namjoo, H. Firouzjahi, and M. Sasaki, *EPL* **101**, 39001 (2013), arXiv:1210.3692 [astro-ph.CO].
- [58] J. Martin, H. Motohashi, and T. Suyama, *Phys. Rev. D* **87**, 023514 (2013), arXiv:1211.0083 [astro-ph.CO].
- [59] T. Suyama, Y. Tada, and M. Yamaguchi, *PTEP* **2020**, 113E01 (2020), arXiv:2008.13364 [astro-ph.CO].
- [60] R. Bravo and G. A. Palma, *Phys. Rev. D* **107**, 043524 (2023), arXiv:2009.03369 [hep-th].
- [61] T. Suyama, Y. Tada, and M. Yamaguchi, *PTEP* **2021**, 073E02 (2021), arXiv:2101.10682 [hep-th].
- [62] C. Germani and T. Prokopec, *Phys. Dark Univ.* **18**, 6 (2017), arXiv:1706.04226 [astro-ph.CO].
- [63] N. Bhaumik and R. K. Jain **10.1088/1475-7516/2020/01/037** (2019), [JCAP2001,037(2020)], arXiv:1907.04125 [astro-ph.CO].
- [64] H. Motohashi and A. A. Starobinsky, *EPL* **117**, 39001 (2017), arXiv:1702.05847 [astro-ph.CO].
- [65] H. Motohashi, A. A. Starobinsky, and J. Yokoyama, *JCAP* **09**, 018, arXiv:1411.5021 [astro-ph.CO].
- [66] V. F. Mukhanov, H. A. Feldman, and R. H. Brandenberger, *Phys. Rept.* **215**, 203 (1992).
- [67] J. Martin, *Braz. J. Phys.* **34**, 1307 (2004), arXiv:astro-ph/0312492.
- [68] J. Martin, *Lect. Notes Phys.* **669**, 199 (2005), arXiv:hep-th/0406011.
- [69] B. A. Bassett, S. Tsujikawa, and D. Wands, *Rev. Mod. Phys.* **78**, 537 (2006).
- [70] L. Sriramkumar, (2009), arXiv:0904.4584 [astro-ph.CO].
- [71] D. Baumann and H. V. Peiris, *Adv. Sci. Lett.* **2**, 105 (2009), arXiv:0810.3022 [astro-ph].
- [72] D. Baumann, in *Theoretical Advanced Study Institute in Elementary Particle Physics: Physics of the Large and the Small* (2011) pp. 523–686, arXiv:0907.5424 [hep-th].
- [73] L. Sriramkumar, On the generation and evolution of perturbations during inflation and reheating, in *Vignettes in Gravitation and Cosmology*, edited by L. Sriramkumar and T. R. Seshadri (World Scientific, Singapore, 2012).
- [74] A. Linde, in *100e Ecole d'Ete de Physique: Post-Planck Cosmology* (2014) arXiv:1402.0526 [hep-th].
- [75] J. Martin, *Astrophys. Space Sci. Proc.* **45**, 41 (2016), arXiv:1502.05733 [astro-ph.CO].
- [76] J. Martin and L. Sriramkumar, *JCAP* **01**, 008, arXiv:1109.5838 [astro-ph.CO].
- [77] G. Tasinato, *JCAP* **03**, 040, arXiv:1411.2803 [hep-th].
- [78] A. Taruya, K. Koyama, and T. Matsubara, *Phys. Rev. D* **78**, 123534 (2008), arXiv:0808.4085 [astro-ph].
- [79] C. Unal, *Phys. Rev. D* **99**, 041301 (2019), arXiv:1811.09151 [astro-ph.CO].

- [80] P. Adshead, K. D. Lozanov, and Z. J. Weiner, *JCAP* **10**, 080, arXiv:2105.01659 [astro-ph.CO].
- [81] M. Taoso and A. Urbano, *JCAP* **08**, 016, arXiv:2102.03610 [astro-ph.CO].
- [82] G. Ferrante, G. Franciolini, A. Iovino, Junior., and A. Urbano, *Phys. Rev. D* **107**, 043520 (2023), arXiv:2211.01728 [astro-ph.CO].
- [83] D. Yamauchi, *PTEP* **2022**, 073E02 (2022), arXiv:2203.15599 [astro-ph.CO].
- [84] G. Franciolini, A. Iovino, Junior., V. Vaskonen, and H. Veermae, *Phys. Rev. Lett.* **131**, 201401 (2023), arXiv:2306.17149 [astro-ph.CO].
- [85] J.-P. Li, S. Wang, Z.-C. Zhao, and K. Kohri, *JCAP* **06**, 039, arXiv:2309.07792 [astro-ph.CO].
- [86] S. Pi, (2024), arXiv:2404.06151 [astro-ph.CO].
- [87] G. Perna, C. Testini, A. Ricciardone, and S. Matarrese, *JCAP* **05**, 086, arXiv:2403.06962 [astro-ph.CO].
- [88] D. Seery, *JCAP* **08**, 018, arXiv:0810.1617 [astro-ph].
- [89] R. R. Caldwell, L. Motta, and M. Kamionkowski, *Phys. Rev. D* **84**, 123525 (2011), arXiv:1109.4415 [astro-ph.CO].
- [90] L. Motta and R. R. Caldwell, *Phys. Rev. D* **85**, 103532 (2012), arXiv:1203.1033 [astro-ph.CO].
- [91] R. K. Jain and M. S. Sloth, *JCAP* **02**, 003, arXiv:1210.3461 [astro-ph.CO].
- [92] R. K. Jain and M. S. Sloth, *Phys. Rev. D* **86**, 123528 (2012), arXiv:1207.4187 [astro-ph.CO].
- [93] K. E. Kunze, *Phys. Rev. D* **87**, 103005 (2013), arXiv:1301.6105 [astro-ph.CO].
- [94] D. Chowdhury, L. Sriramkumar, and M. Kamionkowski, *JCAP* **10**, 031, arXiv:1807.07477 [astro-ph.CO].
- [95] P. J. Sai and R. K. Jain, *JCAP* **09**, 043, arXiv:2307.07502 [hep-th].
- [96] J. M. Maldacena, *JHEP* **05**, 013, arXiv:astro-ph/0210603.
- [97] D. Seery and J. E. Lidsey, *JCAP* **06**, 003, arXiv:astro-ph/0503692.
- [98] X. Chen, *Phys. Rev. D* **72**, 123518 (2005), arXiv:astro-ph/0507053.
- [99] X. Chen, M.-x. Huang, S. Kachru, and G. Shiu, *JCAP* **01**, 002, arXiv:hep-th/0605045.
- [100] D. Langlois, S. Renaux-Petel, D. A. Steer, and T. Tanaka, *Phys. Rev. Lett.* **101**, 061301 (2008), arXiv:0804.3139 [hep-th].
- [101] D. Chowdhury, L. Sriramkumar, and M. Kamionkowski, *JCAP* **01**, 048, arXiv:1807.05530 [astro-ph.CO].
- [102] R. L. Arnowitt, S. Deser, and C. W. Misner, *Phys. Rev.* **117**, 1595 (1960).
- [103] D. Nandi, *JCAP* **08**, 039, arXiv:2103.03159 [astro-ph.CO].
- [104] A. A. Starobinsky and J. Yokoyama, *Phys. Rev. D* **50**, 6357 (1994), arXiv:astro-ph/9407016.
- [105] P. Creminelli and M. Zaldarriaga, *JCAP* **10**, 006, arXiv:astro-ph/0407059.
- [106] N. C. Tsamis and R. P. Woodard, *Class. Quant. Grav.* **26**, 105006 (2009), arXiv:0807.5006 [gr-qc].
- [107] D. Seery, M. S. Sloth, and F. Vernizzi, *JCAP* **03**, 018, arXiv:0811.3934 [astro-ph].
- [108] S. B. Giddings and M. S. Sloth, *JCAP* **01**, 023, arXiv:1005.1056 [hep-th].
- [109] S. B. Giddings and M. S. Sloth, *Phys. Rev. D* **84**, 063528 (2011), arXiv:1104.0002 [hep-th].
- [110] P. Creminelli, J. Noreña, and M. Simonović, *JCAP* **07**, 052, arXiv:1203.4595 [hep-th].
- [111] A. Kehagias and A. Riotto, *Nucl. Phys. B* **864**, 492 (2012), arXiv:1205.1523 [hep-th].
- [112] V. Sreenath and L. Sriramkumar, *JCAP* **10**, 021, arXiv:1406.1609 [astro-ph.CO].
- [113] C. Cheung, A. L. Fitzpatrick, J. Kaplan, and L. Senatore, *JCAP* **02**, 021, arXiv:0709.0295 [hep-th].
- [114] L. Senatore and M. Zaldarriaga, *JCAP* **08**, 001, arXiv:1203.6884 [astro-ph.CO].
- [115] R. J. Ferreira, R. K. Jain, and M. S. Sloth, *JCAP* **10**, 004, arXiv:1305.7151 [astro-ph.CO].
- [116] C. Cecchini and M. Rinaldi, *Phys. Dark Univ.* **40**, 101212 (2023), arXiv:2301.07699 [astro-ph.CO].
- [117] F. Schmidt and M. Kamionkowski, *Phys. Rev. D* **82**, 103002 (2010), arXiv:1008.0638 [astro-ph.CO].
- [118] I. Agullo, D. Kranas, and V. Sreenath, *Front. Astron. Space Sci.* **8**, 703845 (2021), arXiv:2105.12993 [gr-qc].
- [119] B. Das and H. V. Ragavendra, (2023), arXiv:2304.05941 [astro-ph.CO].
- [120] L. Senatore, K. M. Smith, and M. Zaldarriaga, *JCAP* **01**, 028, arXiv:0905.3746 [astro-ph.CO].
- [121] P. A. R. Ade *et al.* (Planck), *Astron. Astrophys.* **594**, A17 (2016), arXiv:1502.01592 [astro-ph.CO].
- [122] Y. Akrami *et al.* (Planck), *Astron. Astrophys.* **641**, A9 (2020), arXiv:1905.05697 [astro-ph.CO].